Corrections of Humidity Measurement Errors from the Vaisala RS80 Radiosonde—Application to TOGA COARE Data

JUNHONG WANG, HAROLD L. COLE, DAVID J. CARLSON, ERIK R. MILLER, AND KATHRYN BEIERLE

National Center for Atmospheric Research, Boulder, Colorado*

ARI PAUKKUNEN

Vaisala OY, Helsinki, Finland

TAPANI K. LAINE

Vaisala Inc., Woburn, Massachusetts

(Manuscript received 27 August 2001, in final form 10 January 2002)

ABSTRACT

A series of laboratory tests have been conducted on several different batches of Vaisala RS80 radiosondes to understand and develop methods to correct six humidity measurement errors, including chemical contamination, temperature dependence, basic calibration model, ground check, sensor aging, and sensor arm heating. The contamination and temperature-dependence (TD) errors dominate total errors. The chemical contamination error produces a dry bias, and is due to the occupation of binding sites in the sensor polymer by nonwater molecules emitted from the sonde packaging material. The magnitude of the dry bias depends on sensor polymer type (RS80-A and RS80-H), age of the sonde, relative humidity (RH), and temperature, and it exists throughout the troposphere. The contamination error generally increases with age and RH, and is larger for the RS80-H than the RS80-A. It is ~2% and ~10% at saturation for 1-yr-old RS80-A and RS80-H sondes, respectively. The TD error for the RS80-A results from an approximation of a linear function of temperature to the actual nonlinear temperature dependence of the sensor, and also introduces a dry bias. The TD error mainly exists at temperatures below −20°C, increases substantially with decreasing temperatures below −30°C, and is much larger for the RS80-A than the RS80-H. The RS80-A's TD correction (C_{TA}) dominates the total correction at temperatures below −40°C and has a correction factor [C_{TA} = (RH)(C_{TA}-factor)] of 0.15, 0.75, and 2.3 at −40°, −60°, and −80°C, respectively.

The correction methods are applied to 8129 Vaisala RS80 soundings collected during the Tropical Ocean and Global Atmosphere (TOGA) Coupled Ocean–Atmosphere Response Experiment (COARE) and are applicable to RS80 radiosonde data from other field experiments and historical and operational radiosonde datasets. The methods are validated by examining various summary plots of the TOGA COARE data and comparing them with other independent data. The corrections greatly improve the accuracy of the TOGA COARE radiosonde dataset. These correction methods have their own uncertainties and may not correct all errors in Vaisala RS80 humidity data. Analyses of these uncertainties are presented in the paper.

1. Introduction

The Tropical Ocean and Global Atmosphere (TOGA) Coupled Ocean–Atmosphere Response Experiment (COARE; in this paper, TOGA COARE will be referred to as COARE), conducted in 1992 and 1993, examined in detail multiscale interactions between the atmosphere and ocean over the warm-pool region of the tropical western Pacific Ocean (Webster and Lukas 1992). As part of enhanced atmospheric monitoring and intensive operations in COARE, a total of 11 540 radiosondes including Vaisala RS80-A, Vaisala RS80-H, and VIZ radiosondes were launched at 42 stations (Fig. 1) in a region that otherwise has relatively little atmospheric sounding data. The COARE radiosonde dataset covers 12 months, and has its highest time and spatial resolution during the COARE intensive operation period (IOP), November 1992 through February 1993. It allows investigators to explore diurnal variations of the boundary layer, convective instability, dry intrusions, synoptic-scale low-level westerly and upper-level easterly wind bursts, and 30–40-day waves. It is also used to calculate atmospheric heat and momentum budgets and, as residuals, surface fluxes. These radiosonde data

* The National Center for Atmospheric Research is sponsored by the National Science Foundation.

Corresponding author address: Dr. Junhong Wang, National Center for Atmospheric Research, Atmospheric Technology Division, P.O. Box 3000, Boulder, CO 80307-3000.
E-mail: junhong@ucar.edu

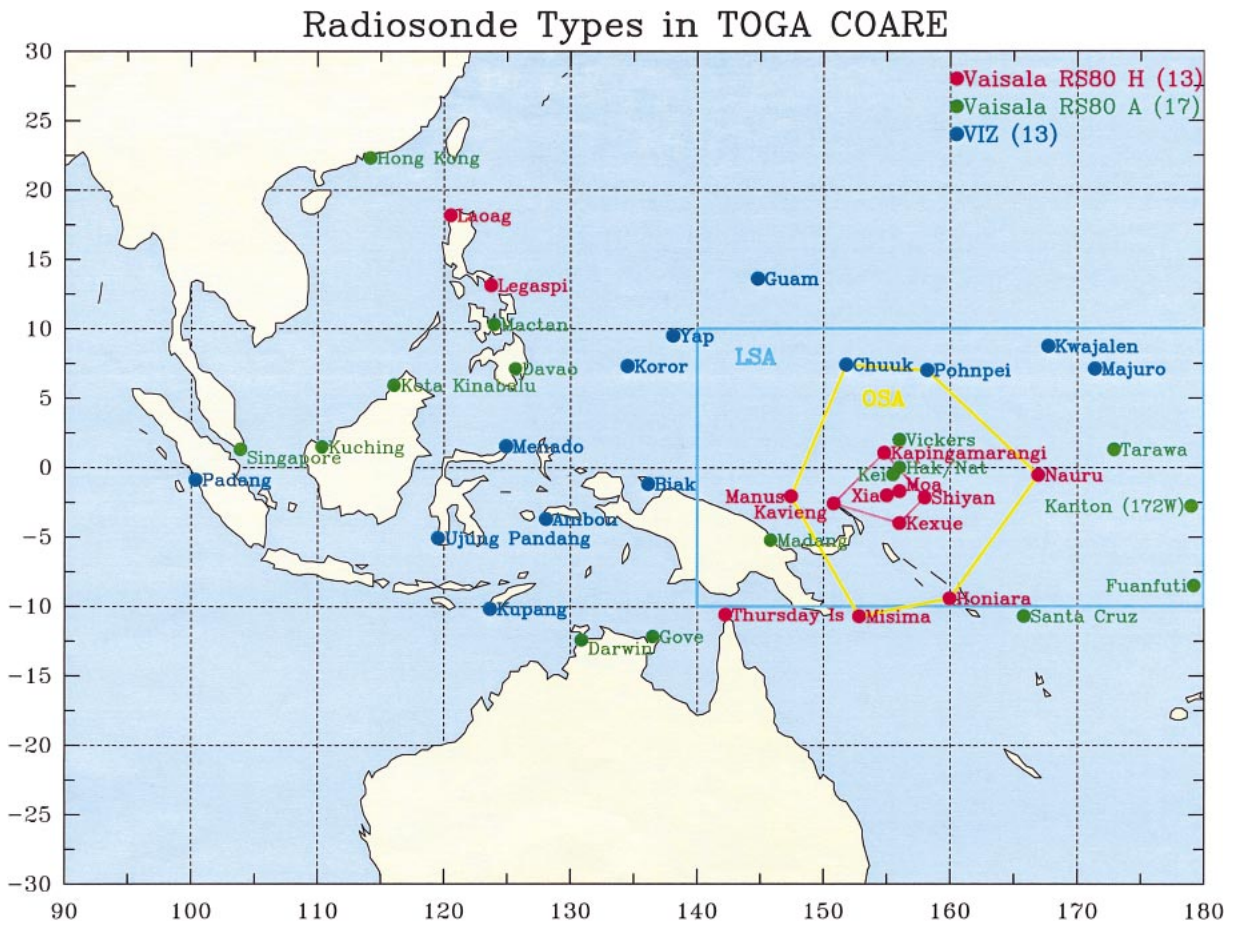

FIG. 1. Geographic distribution of 42 radiosonde stations during TOGA COARE. Station names are colored by radiosonde types (Vaisala RS80-A, Vaisala RS80-H, and VIZ).

also provide unprecedented validation data for various atmospheric and coupled models of tropical processes. Analysis, reanalysis, and modeling efforts worldwide have used and continue to rely on the COARE sounding data.

During COARE operations, several observers expressed surprise at dry boundary layers indicated by radiosonde data. After COARE data collection, Zipser and Johnson (1998, see details in section 3) identified a systematic and significant dry bias in radiosonde humidity data from Vaisala sondes. Use of the original COARE data containing the dry bias can introduce substantial errors in derived radiative and thermodynamical parameters (Guichard et al. 2000) and in calculated atmospheric heat and moisture budgets (Johnson and Ciesielski 2000). In addition, large-scale but probably erroneous spatial variations of moisture evident in composite COARE datasets seem strongly correlated with the geographic distribution of different radiosonde types (e.g., VIZ sondes at sites north of the equator compared to Vaisala sondes used at sites near and south of the equator; see Fig. 4 and the discussion in section 3). Note that the VIZ data were relatively moist, while the Vaisala data were relatively dry (see section 3). When researchers use a numerical weather prediction model to assimilate the full uncorrected COARE dataset, the models can underpredict clouds and precipitation (Lorenc et al. 1996).

More global atmospheric sounding systems use Vaisala radiosondes than any other sondes from any other single manufacturer. Currently, approximately 51% of global operational radiosonde stations and 63% of U.S. stations use Vaisala radiosondes. Globally, most sounding operations use the RS80-A radiosonde first introduced in 1980. Many sounding operations in North America and in the United Kingdom use the RS80-H radiosonde, first introduced in 1992. The use of RS80-H radiosondes during COARE by the Atmospheric Technology Division (ATD) of the National Center for Atmospheric Research (NCAR) represented one of the first large applications of RS80-H radiosondes.

A consequence of the widespread use of Vaisala RS80 radiosondes is that errors or biases in the data can have a large impact on the usefulness of global radiosonde data in weather forecasting, in climate change research, and in calibration and validation of satellite retrieval techniques. Ross and Gaffen (1998) suggested that an apparent tropical atmospheric drying since the late

1980s shown by satellite data calibrated against radiosonde data (Schroeder and McGuirk 1998) occurred largely due to the gradual introduction of faster-response humidity sensors and the replacement of VIZ radiosondes by Vaisala radiosondes at some stations during the 1980s. A separate comparison of global upper-tropospheric humidity from radiosonde data with satellite climatology from the TIROS operational vertical sounder (TOVS) system showed that the relative humidity (RH) in Vaisala RS80-A data is systematically drier than satellite data by ~10% (Soden and Lanzante 1996). Ferrare et al. (1995) compared coincident RH measurements from a Raman lidar and RS80-A radiosondes, and found a consistent dry bias in radiosonde data at all temperatures and RHs. Because Vaisala RS80 radiosondes continue to see widespread use, including use as calibration and comparison tools for satellite and ground-based remote sensing, it seemed important to develop and document a thorough understanding of errors and biases in Vaisala RS80 radiosonde data and to explore correction schemes for important research resources such as the COARE dataset.

Because use of any radiosonde for research purposes can impose more stringent performance goals than typical operational requirements, an effort to improve sensor and sonde data quality for research purposes can result in a substantial improvement for operational usage. Stimulated by the evidence of a systematic dry bias in COARE data, ATD and Vaisala have made substantial efforts, including engineering and laboratory studies and examination of other research datasets, to understand and to correct, physically and via algorithms, errors in Vaisala radiosonde humidity data for both RS80-A and RS80-H sensors. Here we report the development of correction algorithms for both RS80-A and RS80-H sensors and our application of those algorithms to produce a fully corrected COARE dataset. Although developed for high-resolution research data, our correction algorithm will work with any radiosonde data produced by Vaisala RS80 sondes.

We report 1) a series of laboratory tests on RS80-A and RS80-H radiosondes conducted at Vaisala to understand and characterize the dry bias and other errors, 2) the development of physically realistic correction algorithms based on lab tests, 3) application of algorithms to COARE data and validation of algorithms using COARE and other data, and 4) the possibility of applying these algorithms to other radiosonde datasets. We describe the characteristics of and problems in COARE radiosonde data in sections 2 and 3, respectively. We explain six RS80 measurement errors and present corresponding correction methods in section 4. In section 5 we provide an overview of the composite correction algorithm and an analysis of remaining uncertainties. We apply algorithms to all COARE data in section 6, and verify the results by several approaches. Finally, we discuss possible applications of our correction algorithms to other datasets and propose some future applications.

2. Characteristics of TOGA COARE radiosonde data

A total of 11 540 radiosondes were launched at 42 stations in COARE (Fig. 1). Priority stations within the outer sounding array (OSA) launched four sondes per day most of time (0000, 0600, 1200, and 1800 UTC), while the remainder of stations launched two soundings per day (0000 and 1200 UTC). VIZ radiosonde systems were used at 13 stations, accounting for 3411 soundings. The remaining 8129 soundings used Vaisala RS80 radiosondes, including 5581 RS80-H and 2548 RS80-A sondes.

Sounding systems provided by NCAR/ATD, including Integrated Sounding Systems (ISS) (Parsons et al. 1994) and the Cross-Chain Loran Atmospheric Sounding Systems (CLASS), launched 4119 Vaisala RS80 radiosondes at eight stations: Kapingamaraingi, Kavieng, Manus, Nauru, R/V *Moana Wave,* R/V *Kexue,* R/V *Shiyan,* and R/V *Xiangyanghong.* These data, referred to collectively as the NCAR dataset, had some unique and useful characteristics. All NCAR systems launched RS80-H radiosondes except from July to December 1992 at Manus and from July 1992 to January 1993 at Nauru when RS80-A radiosondes were launched. The NCAR systems recorded radiosonde data at the surface prior to launch, an important factor in subsequent error detection and correction. All NCAR systems had associated independent NCAR surface instruments, another important factor in error detection and data correction. Finally, all NCAR data had 1.5-s (~7.5–9 m) vertical resolution and were averaged to 10-s (~50–60 m) resolution.

The rest of the COARE Vaisala RS80 soundings (4010 soundings, referred as non-NCAR data) were launched from standard Vaisala systems. The non-NCAR data were collected at 22 Vaisala stations (17 using RS80-A sensors) including 18 land stations and four research vessels (R/V *Hakuho Maru,* R/V *Natsushima,* R/V *Keifu Maru,* and R/V *Vickers*; Fig. 1). Radiosonde serial numbers and ground check information were recorded at six stations: Darwin, Gove, R/V *Vickers,* R/V *Hakuho Maru,* Misima, and Thursday Island (Table 1). Actual sonde ages (time since manufacture) at these six stations, used later in the dry bias correction (see section 6), can be determined from sonde serial numbers. The non-NCAR soundings had primarily (77%) but not exclusively 10-s resolutions (Table 1). Sensor-arm-heating correction methods described in section 4 can only be applied to 10-s data.

3. Indicators of dry bias in Vaisala radiosonde humidity data

During initial processing of the NCAR sounding data, we recognized that radiosonde temperatures were too warm and humidities too dry in the lowest levels, at least during daytime. These errors were attributed to

TABLE 1. Characteristics of all non-NCAR COARE soundings. The data are categorized by the vertical resolution (10 s, 2 s, variable GTS) and radiosonde types (A and H sondes). In the ''Total'' row, numbers in parentheses are number of soundings.

Category	No. of stations	No. of soundings	Stations with serial numbers recorded	Stations without serial numbers recorded
10-s H sonde	5	1462	Misima, Thursday Island	Laoag, Legaspi, Honiara
10-s A sonde	8	1621	Darwin, Gove, R/V *Vickers*	Tarawa, Madang, Funafuti, Santa Cruz, Hong Kong
2-s A sonde	2	187	R/V *Hakuho Maru*	R/V *Natsushima*
Variable GTS A sonde	5	479		Davao, Kanton, Kota Kinabalu, Kuching, Mactan
Variable A sonde	2	261		Singapore, R/V *Keifu Maru*
Total	22	4010	6 (1346)	16 (2664)

radiational heating of temperature and humidity sensors on the sonde sensor boom, and are referred to as sensor-arm-heating (SAH) error. An algorithm was developed at NCAR/ATD (Cole and Miller 1995) to correct SAH errors. The archived NCAR sounding data at the Joint Office for Science Support (JOSS) at the University Corporation for Atmospheric Research (UCAR) include this correction (see online at http://www.joss.ucar.edu/cgi-bin//codiac/projs?TOGA%20COARE).

Further analysis of COARE sounding data (Zipser and Johnson 1998) showed that the SAH correction had improved temperature and moisture profiles in the lowest 200 m but that a substantial unrealistic dry bias remained evident in NCAR and non-NCAR data collected from both RS80-H and RS80-A radiosondes. Figure 2 shows mean differences between surface water vapor mixing ratio (MR) measured by independent surface instruments and averaged MR near the top of the mixed layer (990–970 mb) measured by radiosondes at 42 stations grouped by radiosonde types. Mean MR differences vary with radiosonde types, with smaller values (<0.5 g kg^{-1}) for VIZ and larger values for RS80-H (Fig. 2). Monin–Obukhov similarity theory would predict differences on the order of 1.0 to 1.25 g kg^{-1} for conditions typical of a well-mixed tropical maritime boundary layer (Fairall et al. 1996). Compared to this expected surface to mixed

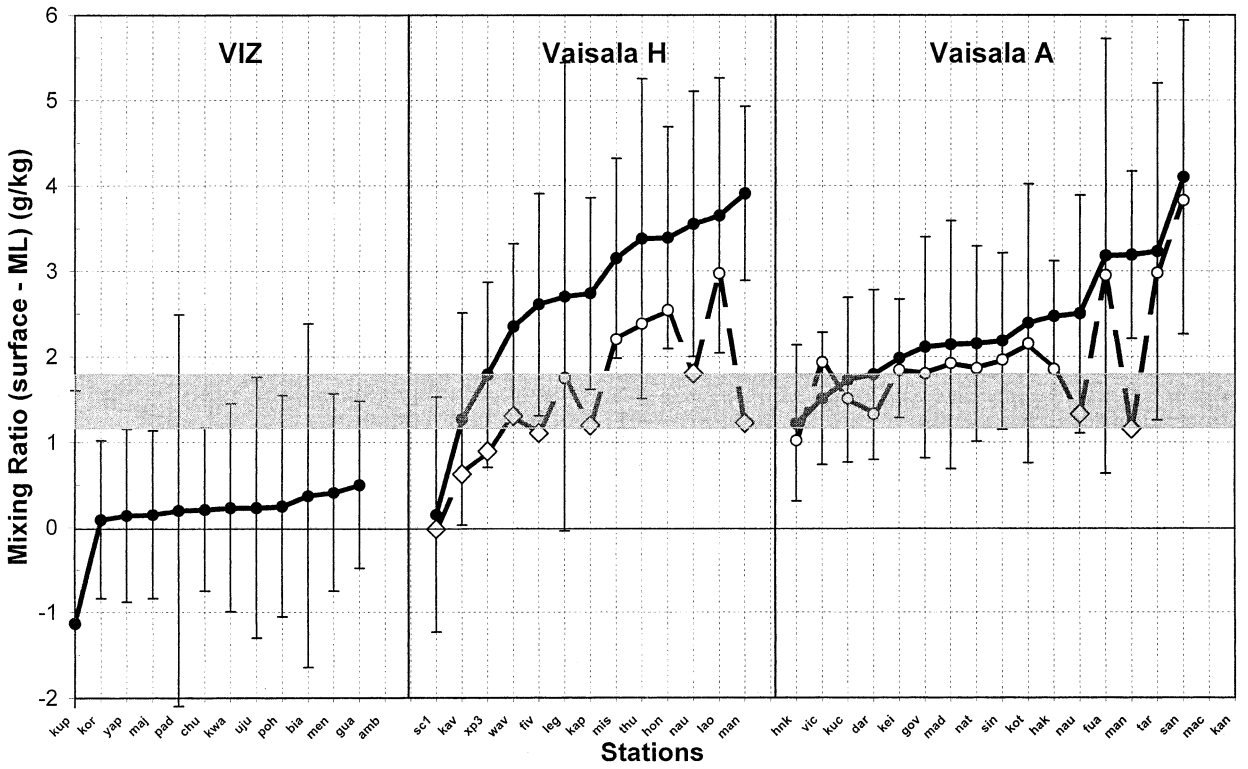

FIG. 2. Mean MR differences (g kg^{-1}) between at the surface and in the mixed layer (ML) at 42 radiosonde stations during TOGA COARE before (solid line with dots) and after (dashed line with diamonds and circles) corrections. For corrected data, diamonds represent using the prelaunch data to make corrections, and circles are using the age method. Station names are represented by the first three letters of full names except that sc1, xp3, fiv, and wav represent R/V *Kexue, Shiyan, Xiangyanghong,* and *Moana Wave*, respectively.

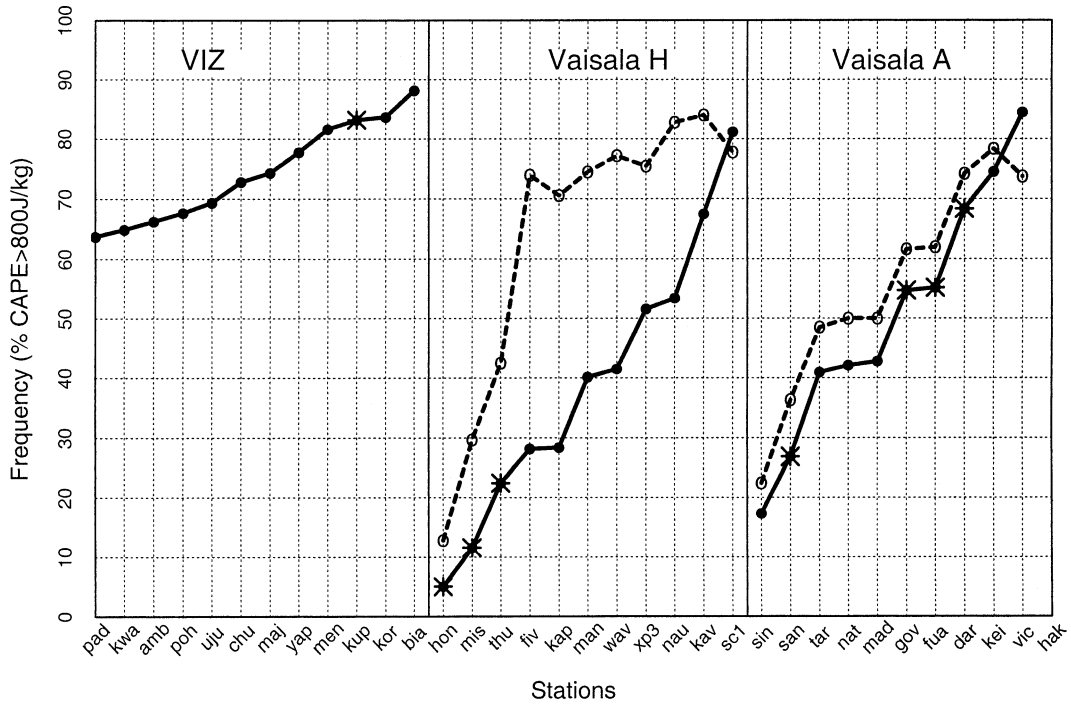

FIG. 3. Frequency (%) of soundings with CAPE larger than 800 J kg^{-1} at 34 radiosonde stations during TOGA COARE before (solid line with dots) and after (dashed line with circles) corrections. Stars are stations around 10°S.

layer MR difference, Fig. 2 suggests a regular pattern of dry biases in Vaisala RS80 radiosonde data from all COARE sounding stations, with larger biases for RS80-H than RS80-A sondes. The uncorrected data in Fig. 2 also show station-specific features, such as small surface to mixed layer differences at R/V *Kexue* (also called ship Science One, or sc1) and Kavieng and a large difference at Santa Cruz. These differences are discussed in more detail in section 6.

Calculations of derived values such as convective available potential energy (CAPE) provide additional evidence that Vaisala sondes used in COARE had a dry bias. Figure 3 shows the frequency of occurrence of soundings at 34 stations during the COARE IOP with CAPE values larger than 800 J kg^{-1}, a value considered as a threshold for convection initiation during the IOP in the COARE region (LeMone et al. 1998). Figure 3 excludes stations with fewer than 20 soundings during the IOP (Kanton, Mactan), stations with data only available at standard pressure levels (Kanton, Kota Kinabalu, Kuching, Mactan), and stations located north of 10°N (Hong Kong, Laoag, Legaspi, Mactan, and Guam). The frequency of CAPE values above 800 J kg^{-1} in uncorrected data was above 60% for all VIZ stations, below 60% for all RS80-H stations except R/V *Kexue* (sc1) and Kavieng (kav) (see section 6), and ranged from 18% to 85% for RS80-A stations (Fig. 3). The contrast among radiosonde types is more apparent if stations located at the same latitude (around 10°S) are chosen (stars in Fig. 3). The data summarized in Fig. 3, coming from large and small islands and from ships and including daytime and nighttime values, suggest limited potential energy available for convection in a region known to have frequent convection and rainfall on small and large scales. The dry biases in Vaisala humidity data, with larger biases for RS80-H than RS80-A, contribute to too low CAPEs in uncorrected COARE sounding data (Fig. 3; Lucas and Zipser 2000; Guichard et al. 2000).

The dry bias in Vaisala humidity data is also revealed in strong latitudinal variations of mean RH profiles derived from TOGA COARE radiosonde data at stations located east of 140°E during IOP (Fig. 4). Figure 4 shows that RHs at low levels are about 10% lower at the south of 5°N than ones between 5° and 10°N. This feature is related with the dry bias in Vaisala measurements and the moist bias in VIZ measurements because at the east of 140°E, VIZ stations concentrate in 5°–10°N, while Vaisala stations dominate the equator and the Southern Hemisphere (Fig. 1).

4. RS80 measurement errors and development of correction methods

The RS80 radiosonde is available with one of two types of the ''Humicap'' capacitive thin-film humidity sensors, the ''A'' or the ''H.'' The Humicap capacitive humidity sensor was developed by Vaisala in the early 1970s (Salasmaa and Kostamo 1975). RS80-A and RS80-H Humicaps differ primarily in properties of the sensor dielectric material. Water vapor is absorbed or

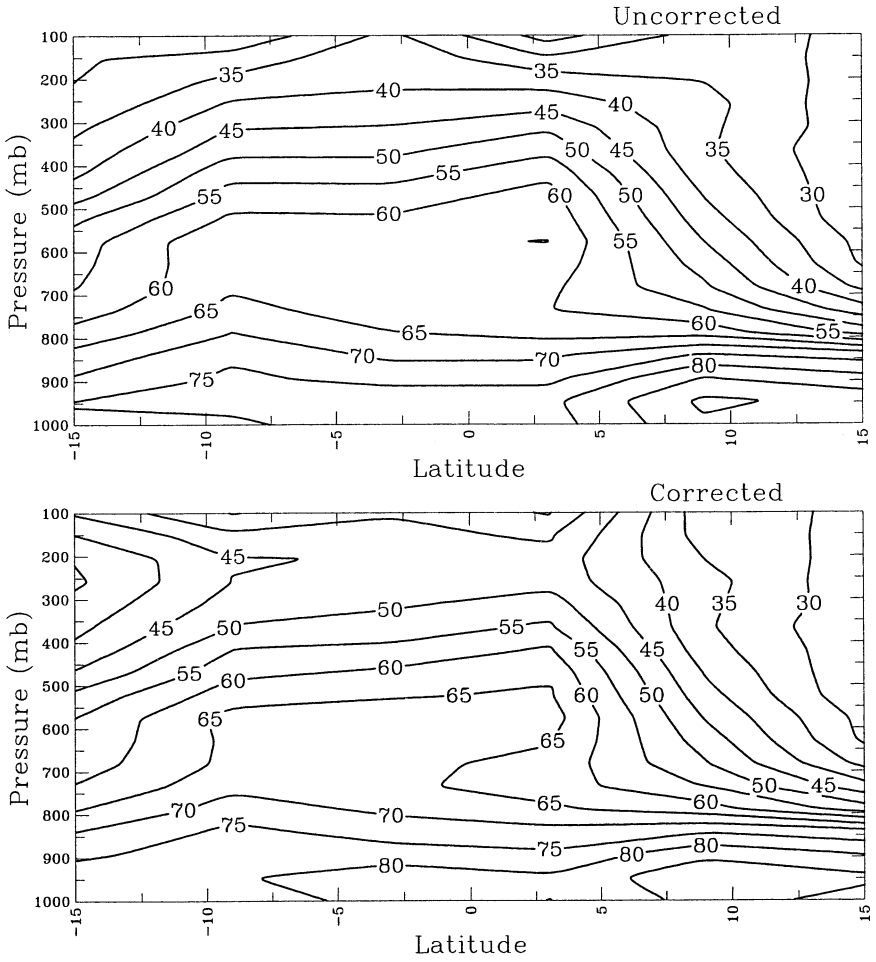

FIG. 4. IOP-mean zonally averaged RH (%) profiles derived from the (top) uncorrected and (bottom) corrected data at stations located at the east of 140°E.

desorbed by the polymer. The polymer layer determines the characteristics of the capacitor in terms of dependence on water vapor and temperature and selectivity and stability to water (Matsuguchi et al. 1998). The A-type polymer material was used as the dielectric for the initial design and is still in use at most radiosonde sites around the world. The H-type polymer sensor was developed and adopted for radiosonde use in the late 1980s. The H sensor is more capable of taking up water, has reduced hysteresis, and is more stable at higher humidities (Antikainen and Paukkunen 1994).

Since the discovery of the dry bias in the Vaisala RS80 humidity data during COARE (Zipser and Johnson 1998), NCAR/ATD has continued to evaluate COARE radiosonde dataset and has collaborated with Vaisala engineers to find reasons for dry biases in both RS80-A and RS80-H sensors. A program was developed to test radiosondes from original COARE radiosonde production batches and from other production batches for different years (Table 2) to study all known humidity error sources. The errors include the dry bias caused by sensor contamination, the basic calibration model error, the short-term calibration drift error, and temperature dependence correction error due to the correction model accuracy. Error correction models were developed based on test results and evaluated using COARE data and other datasets.

a. Chemical contamination error

Contamination was studied in a large test program conducted at the Vaisala manufacturing facility in Helsinki, Finland. Ninety-four stored RS80 radiosondes (Table 2) were tested and analyzed. Tests show that contamination of the polymer material can cause a dry bias in the humidity sensor measurement. Nonwater molecules occupy binding sites, reducing the ability of the polymer to absorb water molecules at these sites that results in a reduced humidity measurement. The source of contaminating molecules is the sonde packaging material that outgasses after the sonde is vacuum-sealed in its Mylar foil bag. The magnitude of the dry bias is a function of the sonde age (i.e., the amount of outgassing that has occurred) and the humidity sensor type. The A-Humicap polymer is less sensitive to contamination

TABLE 2. Characteristics of RS80 radiosondes tested for contamination in Vaisala in 1997. The first 11 batches are RS80-A, and the last 5 batches are RS80-H.

Batch ID no.	No. of sondes	Sonde type	Manufacture date	Ages (yr)	Drying agent
17	8	RS80-30GE	Apr 1997	0.96	Clay I
3	8	RS80-15N	Nov 1996	1.3	Clay I
10	8	RS80-15N	May 1996	2	Clay I
4	8	RS80-15NS	Apr 1995	2.91	Clay I
5	3	RS80-30NS	Nov 1994	3.3	Silica gel II
14	6	RS80-15	May 1993	4.75	Silica gel II
11	4	RS80-15LE	Jan 1993	5.17	Silica gel II
TOGA_A	5	RS80-15L	Jan 1992, Jun 1992	5.5	Clay II
5, 15	9	RS80-30NS RS80-15F	Jan 1992, Mar 1992	6.1	15 clay I, 5 silica gel II
16	7	RS80-18LH	Oct 1997	0.46	Clay I
2	8	RS80-15NH	Dec 1996	1.25	Clay II
7	8	RS80-15LH	Oct 1995	2.5	Clay II
9	8	RS80-18NH	Jun 1996	2.75	Clay I
TOGA_H	4	RS80-15LH	Jun 1992, Feb 1992	5.5	Clay II

than the H-Humicap polymer because of its larger selectivity to water.

The understanding of the contamination stated above and the development of the correction algorithm presented below are based on the following extensive tests.

1) *Accuracy tests.* Accuracy tests were run on 94 radiosondes from 14 different batches that ranged 0.46–6.1 yr old and had been stored in a manner similar to commercial radiosondes (Table 2). The accuracy of these sondes against a traceable reference was measured both before and after the heat treatment. These tests provided information on the magnitude of the contamination error and its change as a function of time.

2) *Heat treatment tests.* Tests measure the amount of the calibration change due to the heat treatment. Before accelerated contamination tests (below), sensors were heated at an increased temperature for several days to remove any previous contamination. Any change in calibration, before and after heat treatment, was attributed to contamination. These tests eliminated any factory-calibration variations from the results because the same calibration coefficients were used before and after heat treatment. It was necessary to eliminate factory-calibration variations because they may cause biases in relatively small test samples even if, in larger quantities, the biases are small.

3) *Tests for sources of contamination.* Sources of contamination were identified by using accelerated contamination tests at increased temperatures and with an increased concentration of sonde packaging materials. The RS80 radiosonde materials were arranged into groups by material types, and amounts of each type of material were increased to produce a high concentration of contaminant sources. The test materials were placed in the normal radiosonde vacuum-storage foil bag with RS80 sensors. These tests identified the styrofoam radiosonde case as the material generating the most contamination. Other plastic components of the radiosonde generated almost as much contamination as the styrofoam. Contamination from these plastic parts was not reduced by desiccant material as effectively as contamination from styrofoam. The RS80-A polymer seemed to react less to the styrofoam contamination than the RS80-H polymer.

4) *Preventive action tests.* A series of tests were run using different absorbing materials that could be placed in the sealed radiosonde storage bags. These tests found that by changing the absorbing material from clay to a mixture of activated charcoal and silica gel the contamination was reduced by 30%–50%. This new desiccant mixture along with a mechanical contamination shield was introduced in April 1998, and has been used in production since September 1998 for all RS80 radiosondes. Further modification involved enclosing the sensor boom with a specially sealed cover that also contains some of the new absorbing material. This new cover is made of a special low out-gassing plastic material. This change is expected to prevent any remaining contamination. The sensor boom cover was introduced in May 2000 for RS80 radiosondes and was incorporated into production in June 2000.

The average contamination for different batches of sondes (Table 2) as a function of age and RH was calculated from the test data. A polynomial fit was applied to the average contamination, and a correction model for contamination was derived. The contamination corrections (in %) of the basic calibration models for RS80-A (C_{CA}) and RS80-H (C_{CH}) sensors are

$$C_{CA} = [ka_0 + (ka_1)(d) + (ka_2)(d^2)] \times [pa_0 + (pa_1)(U) + (pa_2)(U^2) + (pa_3)(U^3)] \quad (4.1\text{-A})$$

$$C_{CH} = [kh_0 + (kh_1)(d) + (kh_2)(d^2) + (kh_3)(d^3) + (kh_4)(d^4)] \times [ph_0 + (ph_1)(U) + (ph_2)(U^2) + (ph_3)(U^3)] \quad (4.1\text{-H})$$

where d is the sonde age in years, U is the relative humidity in percent indicated by the basic calibration of the sensor (different from the measured RH; see section 4b). In Eq. (4.1) and subsequent equations, the A refers to the RS80-A sonde and H to the RS80-H. Coefficients ka_i, pa_i, kh_i, and ph_i, respectively, are derived from the polynomial fit

$ka_0 = 0.066\,704 \quad ka_1 = 0.391\,14$

$ka_2 = -0.040\,26$

$pa_0 = 0.6678 \quad pa_1 = 0.0854 \quad pa_2 = 0.0004$

$pa_3 = -1.0013\text{E-}5$

$kh_0 = 0.018\,866 \quad kh_1 = 1.978\,206$

$kh_2 = -1.34278 \quad kh_3 = 0.369\,157\,24$

$kh_4 = -0.032\,41$

$ph_0 = 1.6994 \quad ph_1 = 0.1368 \quad ph_2 = -0.0018$

$ph_3 = 1.4105\text{E-}5.$

Note that $pa_0 = 0$ and $ph_0 = 0$ if the modeled or observed ground-check correction is used (see sections 4e and 4f). All RHs and corrections to RH used in this paper are given in percent (%). The correction is a function of the sonde age, RH, and temperature (Fig. 5). This correction generally increases with age and RH and is ~2% and ~10% at saturation for 1-yr-old RS80-A and RS80-H sondes, respectively. The RS80-A has a much smaller contamination correction than the RS80-H.

If there is no age information available (i.e., serial numbers are not recorded), the contamination error can be corrected using the surface RH measured by an independent surface instrument ($U_{\text{surf\_ref}}$) and by the radiosonde prior to the launch ($U'_{\text{surf\_sonde}}$) if they are recorded. The surface RH difference between $U_{\text{surf\_ref}}$ and $U'_{\text{surf\_sonde}}$ is considered as the combination of the contamination dry bias and the SAH error in the radiosonde data. After excluding the SAH error, the contamination correction at the surface is obtained and is substituted in Eqs. (4.1-A) and (4.1-H) to obtain the age term in (4.1-A) and (4.1-H). As a result, the contamination correction for the RS80-A (4.2-A) and for the RS80-H (4.2-H) is:

$$C_{\text{CA}} = \Delta U_{\text{surf}}\left[\frac{pa_0 + (pa_1)(U) + (pa_2)(U^2) + (pa_3)(U^3)}{pa_0 + (pa_1)(U_{\text{surf\_sonde}}) + (pa_2)(U^2_{\text{surf\_sonde}}) + (pa_3)(U^3_{\text{surf\_sonde}})}\right] \tag{4.2-A}$$

$$C_{\text{CH}} = \Delta U_{\text{surf}}\left[\frac{ph_0 + (ph_1)(U) + (ph_2)(U^2) + (ph_3)(U^3)}{ph_0 + (ph_1)(U_{\text{surf\_sonde}}) + (ph_2)(U^2_{\text{surf\_sonde}}) + (ph_3)(U^3_{\text{surf\_sonde}})}\right], \tag{4.2-H}$$

where U is RH at the basic calibration temperature, $\Delta U_{\text{surf}} = U_{\text{surf\_ref}} - U'_{\text{surf\_sonde}} - \Delta U_{\text{SAH}}$, and $U_{\text{surf\_sonde}}$ is the surface sonde RH at the basic calibration temperature, and is derived from $U'_{\text{surf\_sonde}}$ using correction equations (5.1-A) for the RS80-A and (5.1-H) for the RS80-H. Here, ΔU_{SAH} is the SAH error at the surface (see section 4d).

b. Temperature dependence error

Relative humidity is derived from measured sensor capacitance for the Humicap. The sensor calibration and RH calculation are done in two phases. In the first phase, RH is calculated from the basic calibration equation by using individual calibration coefficients, which is called as RH at basic calibration temperature and referred as U in all equations (and in Figs. 10 and 11). In the second phase, the temperature dependence (TD) correction model is applied to U to derive the measured RH at the ambient temperature (U'). Temperature dependence correction models for the RS80-A and the RS80-H are the following:

$$U' = \frac{U + 2.221\,68 - 0.111\,08t}{0.999\,634 + (1.831\,05\text{E-}5)t} \tag{4.3-A}$$

$$U' = \frac{U + 0.61 - 0.031t + 0.000\,33t^2 + 0.000\,001\,4t^3 + (3.1\text{E-}9)t^4}{0.9561 + 0.003\,59t - 0.000\,072\,7t^2 - (9.6\text{E-}8)t^3 + (5.431\text{E-}9)t^4}, \tag{4.3-H}$$

where t is the ambient temperature in degrees Celsius. The temperature dependence of sensors is nonlinear by nature, but the TD correction model used for the RS80-A sensor is a linear function of temperature (4.3-A) causing an error (referred to as the TD error). For RS80-A, the TD error is the difference between the old TD

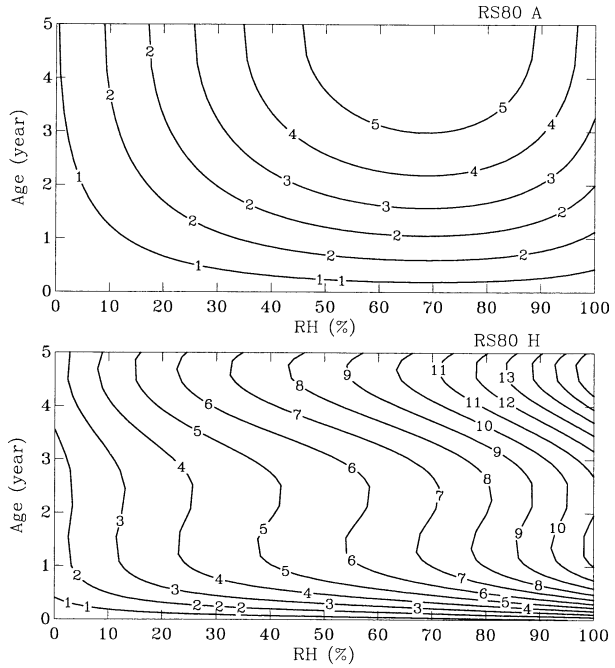

FIG. 5. The contamination corrections (%) as a function of sonde age and RH for (top) RS80-A and (bottom) RS80-H at the basic calibration temperature.

correction model (4.3-A) and the new model derived from laboratory measurements at Vaisala (Miloshevich et al. 2001). The TD correction for the RS80-H sensor is based on improved TD correction model (4.3-H). Note that the TD correction model is used to derive RH at the ambient temperature from basic calibration RH, and the correction for the TD error discussed here is used to correct the error in the TD correction model and is referred as the TD correction. The correction of the TD error is different for RS80-A and RS80-H sensors, and is described separately below.

1) THE RS80-A HUMIDITY SENSOR

The estimation of the correction for the RS80-A TD error is based on data from tests at a saturation humidity level at a series of temperatures (Miloshevich et al. 2001). The measured RH differences were fitted by a polynomial to derive the correction at saturation level C'_{TA}:

$$C'_{TA} = C_0 + C_1 t + C_2 t^2 + C_3 t^3 + C_4 t^4 + C_5 t^5 \quad (4.4)$$

where t is the ambient temperature in degrees Celsius, and derived polynomial coefficients are $C_0 = 0.3475$, $C_1 = 0.0283$, $C_2 = 4.2090\text{E-}4$, $C_3 = -1.4894\text{E-}4$, $C_4 = 6.4325\text{E-}7$, $C_5 = 2.1677\text{E-}8$. The correction at humidity levels lower than saturation is done by using a linear interpolation from 0% correction at 0% RH. The TD correction model is expected to be accurate enough at 0% RH, so there is no TD error at 0% RH. The correction for all humidity levels C_{TA} is

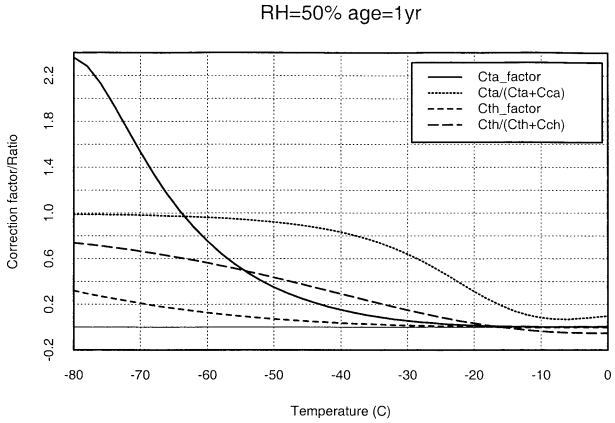

FIG. 6. The TD correction factor (C_{TA} factor and C_{TH} factor) as a function of temperature for RS80-A and RS80-H. The ratio of TD correction (C_{TA} and C_{TH}) to the sum of TD and contamination corrections (C_{CA} and C_{CH}) at 50% RH and for a 1-yr-old sonde is also presented.

$$C_{TA} = \left[\frac{U' + \dfrac{C_{CA} + C_{MA}}{0.999\,634 + (1.831\,05\text{E-}5)t}}{U_{MAX} - C'_{TA}}\right] C'_{TA}$$

$$= \left(\frac{U'_C}{U_{MAX} - C'_{TA}}\right) C'_{TA}, \quad (4.5)$$

where C_{MA} is the correction for the basic calibration model error (see section 4c), U_{MAX} is the saturation RH with respect to water (where $U_{MAX} = 99.8526 + 0.9442t + 0.0034t^2$ if $t < 0$°C and $U_{MAX} = 100$ if $t >= 0$°C), and U'_C is the RH corrected for contamination and the basic-calibration-model errors [see Eqs. (5.2-A and -H) and Figs. 10 and 11]. The correction factor $[C'_{TA}/(U_{MAX} - C'_{TA})]$ increases substantially with decreasing temperatures, and is 0.15, 0.75, and 2.3 at −40°, −60°, and −80°C, respectively (Fig. 6). The contamination correction and the correction for the TD error are two major components of the total correction for the RS80-A sensor. The TD correction dominates total correction at temperatures below −40°C (>80% of total; Fig. 6).

2) THE RS80-H HUMIDITY SENSOR

A similar saturation level test has been applied to RS80-H sondes. Instead of correction equations similar to (4.4) and (4.5), a new temperature dependence model was derived for the RS80-H. The correction for the RS80-H TD error is done by applying new coefficients to the TD correction model (4.3-H). The new TD correction model is used to convert basic calibration RH (after correction for contamination and basic-calibration-model errors) to RH at ambient temperature (U'_C; see section 5a). The TD error for the RS80-H is much smaller than that for the RS80-A (Fig. 6). The TD correction factor for the RS80-H has a maximum value of 0.3 at −80°C.

c. Basic calibration model error

All Vaisala radiosonde humidity sensors are individually calibrated during production. Each sensor is measured against a reference, and the basic calibration model is fitted through these calibration points. This determines the individual basic calibration curve for each humidity sensor. The humidity sensor's temperature dependence is checked at −30° and 45°C during calibration. The calibration error originates from applying an averaged basic calibration model or an averaged temperature dependence model to each sensor. An accurate test chamber with traceable references was used to generate reference humidity values for tests of the basic calibration model error at 20%, 50%, 70%, 80%, and 90% RH at Vaisala. The tests show that both RS80-A and RS80-H sensors read too moist at RH above ~70%. The basic calibration model corrections for the RS80-A and the RS80-H, C_{MA} and C_{MH}, were derived by applying a polynomial fit to the test data:

$$C_{MA} = A_0 + A_1U + A_2U^2 + A_3U^3 + A_4U^4 \quad (4.6\text{-A})$$

$$C_{MH} = H_0 + H_1U + H_2U^2 + H_3U^3, \quad (4.6\text{-H})$$

where $A_0 = 0.0143$, $A_1 = -0.3677$, $A_2 = 0.019$, $A_3 = -0.000\ 297\ 91$, $A_4 = 1.4298\text{E-}6$, $H_0 = -0.3019$, $H_1 = -0.0081$, $H_2 = 0.0011$, and $H_3 = -1.23\text{E-}5$. In our correction algorithm described in section 5, we removed the basic-calibration-model correction, that is, $C_{MA} = 0$, and $C_{MH} = 0$. The argument for removing the correction is that in the laboratory where the model correction was developed, the sensors were placed in a humidity chamber and stabilized for long periods (e.g., 30–60 min). Over that time period, the sensor drifts upward and reads too moist at high humidity. However, during balloon ascent in the real atmosphere, humidity changes quickly, and the sensor does not have time to drift upward unless it is in a cloud for a long period of time.

d. Sensor-arm-heating error

The SAH error is attributed to the daytime radiational heating of the humidity sensor arm prior to launch. The heated sensor arm results in a high saturation vapor pressure and leads to an erroneously low RH measurement. The SAH effect persists through the first 40–60 s (200–300 m) of the sounding and diminishes with time (height) because of the ventilation of the sensor arm as the radiosonde ascends. The sensor arm reaches thermal equilibrium with the environment in approximately three thermal time constants (i.e., the time constant is ~13 s for the sensor arm). The SAH also impacts temperature measurements, but its effect is negligible because of the small thermal time constant of the temperature sensor (~2 s). A correction method for the SAH error was developed at NCAR (Cole and Miller 1995) and applied to NCAR daytime COARE soundings. It was found that the method erroneously assumed that total difference in RH measured by the independent surface instrument and by the radiosonde prior to launch was due to the SAH. Total surface RH difference is in fact a combination of the contamination dry bias and the SAH error. Here, we revised the method by estimating the SAH component using the prelaunch sonde temperature and the surface temperature measured by the independent surface instrument (Cole and Miller 1995). The SAH error at the surface (ΔU_{SAH}) is

$$\Delta U_{SAH} = U_{surf\_ref} - \frac{U_{surf\_ref} e_s(T_{surf\_ref})}{e_s(T_{surf\_sonde})}, \quad (4.7)$$

where U_{surf_ref} and T_{surf_ref} are RH (%) and temperature (°C) measured by the surface independent instrument, T_{surf_sonde} is temperature (°C) measured by the radiosonde prior to launch, and e_s is the saturation vapor pressure (in mb). Note that e_s (T_{surf_ref}) is e_s at T_{surf_ref}. The SAH correction is applied to the first 50 s of data by using the following equation:

$$\Delta U_{SAHi} = (\Delta U_{SAH}) e^{-t_i/13}, \quad (4.8)$$

where t_i is the time (s) at the first 50 s, and 13 is the thermal time constant of the humidity sensor arm. The old SAH correction was removed from the NCAR sounding data and the new correction was applied. In general, a temperature difference of 1°C between the ambient and the sensor arm is equal to ~4% SAH error in RH.

The SAH correction scheme used for the NCAR sounding data requires the prelaunch radiosonde temperature and humidity data with high vertical resolution (1.5 s for COARE data), which are not available for the non-NCAR data. Therefore, a statistical correction method was developed based on the NCAR sounding data. The basis for the statistical approach is that the radiosonde-measured RH at 10 s (the vertical resolution of most soundings, ≤50 m; Table 1) in a well-mixed boundary layer should be about the same as the surface RH measured by the surface instrument (RH_{sfc}) unless a low-level inversion occurs, or there are errors in the radiosonde data. Therefore, if the RH at 10 s (RH_{10s}) has been corrected for the contamination dry bias along with other errors described previously, then the SAH error is approximately equal to $RH_{sfc} - RH_{10s}$. The SAH error at 10s (ΔU_{SAH_10s}) for the NCAR data is derived from that at the surface (ΔU_{SAH}), $\Delta U_{SAH\_10s} = (\Delta U_{SAH})\, e^{-10/13}$. Figure 7 shows the relation between RH_{sfc} minus RH_{10s} corrected for the dry bias along with other errors (U'_c in Fig. 11, referred to as ΔU) and ΔU_{SAH} for 1033 daytime NCAR soundings at five stations. The data on the R/V *Kexue* were excluded in Fig. 7 because of condensation effects, and the soundings at Kapinga and Nauru were also excluded because there were no SAH errors (see section 6). Ninety-three percent of the soundings have ΔU larger than 0%, suggesting another dry bias in the RH_{10s} data (e.g., SAH) beside the contamination dry bias and the TD error. The correlation coefficient between ΔU and ΔU_{SAH} is 0.64, and is above

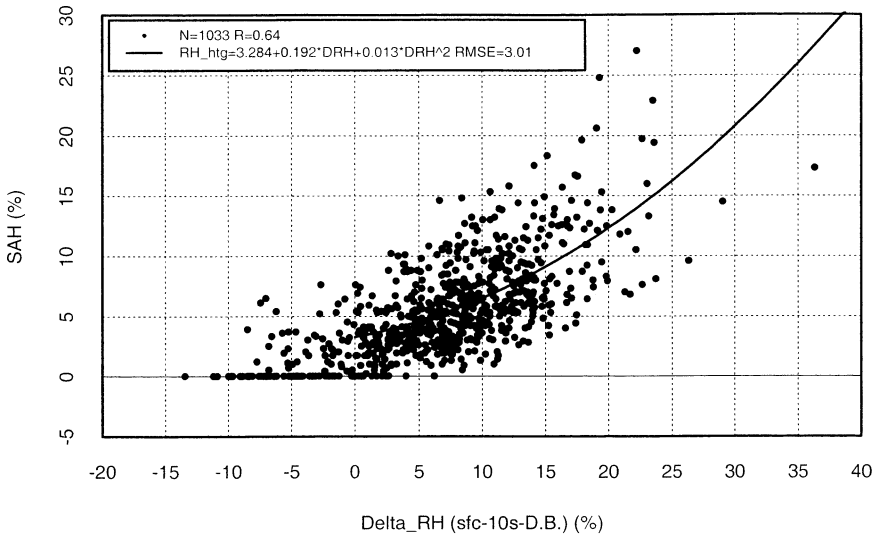

FIG. 7. Scatterplot of SAH errors vs the surface RH from surface instrument minus radiosonde-measured RH at 10 s after corrections of the contamination dry bias along with other errors (D.B. in *x*-axis label) from 1033 NCAR soundings. The linear correlation coefficient between two is 0.64. The solid line is the third-order polynomial fit to the data.

the 99% significance level, indicating the possibility of predicting ΔU_{SAH} from ΔU (Fig. 7). A third-order polynomial fit is applied to the data and gives a root-mean-square error of 3% (Fig. 7). The SAH error for non-ATD soundings is derived from ΔU using the following equation:

$$\Delta U_{\mathrm{SAH}} = 3.284 + 0.192\Delta U + 0.013\Delta U^2. \quad (4.9)$$

The SAH correction is applied to the first 50 s of data by using (4.8). Note that this SAH correction scheme can only be applied to non-NCAR soundings with 10-s vertical resolution.

e. Ground-check error

The ground-check (GC) correction for Vaisala radiosonde measurements is an on-site calibration in temperature, relative humidity, and pressure prior to launch based on radiosonde measurements at reference values. Ground-check corrections are applied to the entire radiosonde profile although the procedure provides a calibration at only certain reference values. The humidity GC correction is based on the sonde measurement at 0% reference RH by inserting the radiosonde humidity sensor (Humicap) into a desiccant box. The desiccant is used to dry the air inside the box to 0% RH. The RH GC correction is the difference between the reference RH (0%) and the measured RH. GC corrections are designed to remove possible biases and/or errors of radiosonde instruments before launch. However, human errors, contamination, degradation of GC instruments with age, and other factors can introduce errors in GC corrections (Kostamo 1989; Lesht 1995; Wang et al. 2000). As a result, GC corrections do not necessarily improve radiosonde measurement accuracy, and are likely in some cases to reduce it if not made properly.

During TOGA COARE, GC corrections were performed at some stations, and the correction data are available at Darwin, Misima, Thursday Island, Gove, the R/V *Hakuho Maru* and the R/V *Vickers*. The histograms of RH–GC corrections during TOGA COARE show moist biases in the Vaisala humidity sensor at Darwin, Misima, and Thursday Island for 59%, 50%, and 34% of all soundings, respectively (Fig. 8). However, radiosondes used at Gove and on the *Vickers* had dry biases with a mean of 1.23% and 2.09%, respectively. It is expected that RH–GC corrections would be positive values with a distribution similar to that at Gove and on the *Vickers*, representing the humidity sensor's dry bias due to contamination and normal aging. The soundings on the *Vickers* show a very small dry bias, suggesting that GC corrections can help remove the bias in the data in some cases.

The possible explanation for the moist bias at Darwin, Misima, and Thursday Island shown in Fig. 8 could be old desiccant or human error. In a moist environment, such as in the Tropics where COARE was conducted, the reference RH value can be above 0% if the chamber containing the desiccant is contaminated by moisture from the outside, and/or the desiccant has deteriorated. In either case, GC software will still interpret the reference RH as 0%. The radiosonde-measured RH could also be above 0% if the operator does not allow the RH sensor to stay in the chamber long enough to dry to 0%, and/or the old desiccant is incapable of drying the air inside the chamber to 0%. As a result, the RH–GC correction (reference sonde) could be negative. The operator is

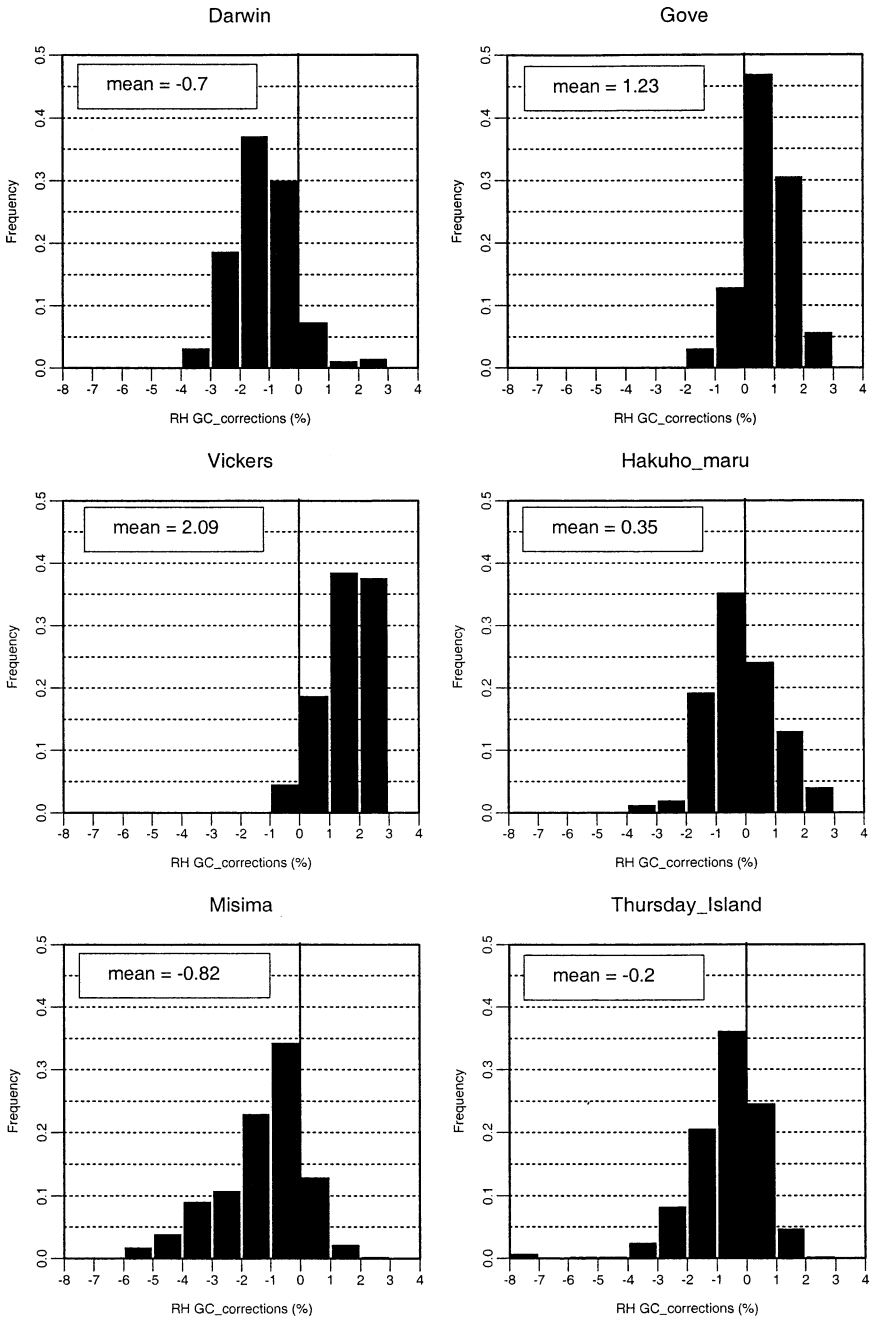

FIG. 8. Frequency distributions of RH–GC corrections (%) at six stations. The mean value at each station is also given in the plot.

responsible for inspecting the desiccant and changing it as soon as its color has started to change from blue to gray; however, this does not always happen because operators either do not notice the desiccant color change, or they are not familiar with the proper operating procedure. The time evolution of RH–GC corrections at Misima in Fig. 9 shows the largest moist biases from 19 January to 11 February 1993 and reasonable values suddenly afterward. The RH–GC correction changes from −6% at 1049 UTC to 1% at 1643 UTC on 11 February 1993. The possible explanation is that the old desiccant was replaced on 12 February 1993. Based on this analysis, we remove GC corrections at these six stations ($\Delta U'_{\rm GC}$) before making any other corrections (see section 6). Therefore, U' used in calculations should be measured RH (U_m) minus $\Delta U'_{\rm GC}$:

$$U' = U_m - \Delta U'_{\rm GC}. \qquad (4.10)$$

f. Sensor aging error

Another type of the dry bias error is caused by long-term instability of the sensor, referred to as the ''sensor aging.'' The A sensor is unstable and drifts more during storage than the H-polymer sensor. The long-term stability is monitored by Vaisala's factory quality control. The drift is mainly caused by reduced polymer sensitivity to water vapor, and is therefore seen more clearly at high humidities. The A-Humicap drift at saturation is approximately −5% RH (dry) after a 2-yr storage time, and less than −0.5% RH per year thereafter. The drift can be partially eliminated prior to launch using the GC correction. However, due to problems in GC corrections discussed above and no GC corrections at some stations, a modeled GC correction as a function of sonde age (d) for both the RS80-A and the RS80-H, ΔU_{GC_A} and ΔU_{GC_H}, has been derived from the after-baking data taken during laboratory tests:

$$\Delta U_{GC\_A} = 0.0666 + 0.8d - 0.104d^2 \quad (4.11\text{-A})$$

$$\Delta U_{GC\_H} = -0.1638 + 1.4766d - 0.2257d^2, \quad (4.11\text{-H})$$

where d is the sonde age in years. We applied the modeled GC correction to all COARE soundings (see section 5).

5. Correction algorithm and uncertainty analysis

a. Overview of correction algorithm

Six major errors in Vaisala RS80 humidity data have been explained above, and the correction method for each error was also presented. The flowcharts in Figs. 10 and 11 show the correction algorithm using the sonde age and the prelaunch radiosonde data, respectively. The basic calibration RH (U) is used for the contamination and basic calibration model corrections, and calculated from the measured RH (U_m) after removing the measured GC correction (4.10) using the following Eq. (5.1-A) for the RS80-A and (5.1-H) for the RS80-H:

$$U = -2.221\,68 + 0.999\,634U' + [0.111\,08 + (1.831\,05\text{E-}5)U']t \quad (5.1\text{-A})$$

$$U = -0.61 + 0.9561U' + (0.031 + 0.003\,59U')t + (-0.000\,33 - 0.000\,072\,7U')t^2 + [-0.000\,001\,4 - (9.6\text{E-}8)U']t^3 + [(-3.1\text{E-}9) + (5.431\text{E-}9)U']t^4, \quad (5.1\text{-H})$$

where t is the ambient temperature in degrees Celsius and U' is obtained from Eq. (4.10). The sonde age (d) is needed for contamination and modeled GC corrections in the correction algorithm using the sonde age (Fig. 10). If serial numbers are recorded in the data, the sonde age can be accurately calculated. Otherwise, a manufactured date is assumed for TOGA COARE data (see section 6a), and the sonde ages are calculated. Note that all sondes used at one station are assumed to be manufactured on the same date, which is not necessarily true (see section 6a). The basic calibration RH (U) is first derived from (5.1), then is corrected for contamination and basic-calibration-model errors (U_C; see Figs. 10 and 11), and finally it is then corrected back to RH at ambient temperature (U'_C):

$$U'_c = \frac{U_c + 2.221\,68 - 0.111\,08t}{0.999\,634 + (1.831\,05\text{E-}5)t} \quad \text{for the RS80-A} \quad (5.2\text{-A})$$

$$U'_c = \frac{U_c + 0.61 - 0.031t + 0.000\,33t^2 + 0.000\,001\,4t^3 + (3.1\text{E-}9)t^4}{0.9601 + 0.003\,59t - 0.000\,085\,7t^2 + (9.3\text{E-}8)t^3 + (6.931\text{E-}9)t^4} \quad \text{for the RS80-H,} \quad (5.2\text{-H})$$

where t is the ambient temperature in degrees Celsius. The TD correction (C_{TA}) for the RS80-A is calculated from (4.5), and is applied to U'_C along with the modeled GC correction (ΔU_{GC_A}). For the RS80-H, the correction for the TD error has been incorporated in (5.2-H) by using the new coefficients for the TD correction model. During the daytime, Eqs. (4.7), (4.8), and (4.9) are used to correct the SAH error. Finally, the corrected RH (U_{mC}) is obtained. The dewpoint temperature and altitude are recalculated using the corrected RH. The impact of corrections on dewpoint temperature depends on temperature and RH, and is less than 4°C at RH > 30% if the correction is smaller than 10%. The impact on altitude is negligible (<1 m).

b. Uncertainty analysis

The contamination, TD, basic calibration model, and modeled GC corrections are all polynomial fits to the data from a limited number of laboratory tests for a limited number of sorides, and bear some uncertainties because of uncertainties in the test data. This uncertainty is called as the model uncertainty hereafter. The uncertainty of the statistical SAH correction method is a result of scatters shown in Fig. 7, and is the root-mean-square error of the polynomial fit (3.01%). In addition, if there is no serial number information available, assumed ages can also introduce uncertainties in the contamination and modeled GC corrections (called as the age uncertainty hereafter). The uncertainty in each correction at

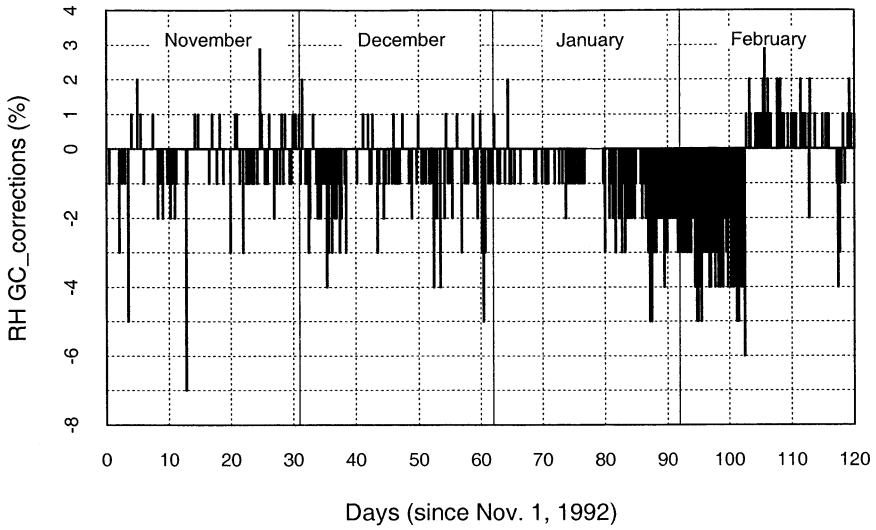

FIG. 9. Time series of RH–GC corrections (%) at Misima from 1 Nov 1992 to 28 Feb 1993.

an ambient condition of 27°C and 80% RH is summarized in Table 3 for a 0.96-yr-old RS80-A sonde and in Table 4 for a 1.25-yr-old RS80-H sonde. The reason for choosing different ages for RS80-A and RS80-H sondes is to be consistent with sonde ages tested in the laboratory (see Table 2).

The largest model uncertainty comes from the statistical SAH correction model in the absolute value (3.01%). For relative values, however, the largest uncertainty occurs for the contamination correction model for the RS80-A (90%), and for the basic calibration model for the RS80-H (285%). The uncertainty in the SAH correction model is the maximum at the surface (3.01%), and decreases to 1.39% at 10 s. For contamination and modeled GC corrections that are dependent on age, uncertainties due to a 50% uncertainty in age are smaller than 50% (relative), and less than or have the same magnitude as model uncertainties for both the RS80-A and the RS80-H. The age uncertainty in the contamination correction is shown in Fig. 12 as a function of RH, and is less than 45% for all sondes younger than 2 yr old. After removing the basic-calibration-model correction, total uncertainty is decreased, especially for the RS80-A. This supports our decision to remove the basic-calibration-model correction from our correction model discussed in section 4c. Total model uncertainty is larger than the age uncertainty, and is 87% and 81% of total uncertainty for RS80-A and RS80-H, respectively.

All six errors described in section 4 except basic calibration model error produce dry biases rather than random errors. Total uncertainty of correction methods after removing basic calibration model correction is smaller than total correction for both the RS80-A and the RS80-H (Tables 3 and 4). It implies that our correction model always produce a dry bias correction ($C_{\mathrm{TOTrmCm}} \pm \Delta C_{\mathrm{TOT}}$ in Tables 3 and 4) despite its uncertainty and thus acts to improve the accuracy of radiosonde data. The evaluation of our correction methods using COARE data in section 6c also shows the improved accuracy in corrected radiosonde data. Our overall uncertainty analysis of methods shows the usefulness of those correction methods as well as some limitations.

Besides model and age uncertainties discussed above, the contamination correction may also have uncertainties due to ignoring the influence of the two different drying agents, clay and silica gel, and any contaminant from the storage bag itself. Some other known errors are not included in our correction methods, such as solar radiation errors, factory calibration variability (batch-to-batch difference), and sensor time lag errors. There might be some solar heating of the humidity sensor because the sensor boom and the plastic cap over the humidity sensor are aluminized, but still have a solar absorptivity of about 12%. The sensor heating due to solar radiation is about 0.5°C in the troposphere, corresponding to about 5% RH maximum at saturation. Significant batch-to-batch differences in the radiosonde humidity data are found in the atmospheric radiation measurement (ARM) program (Lesht 1999). The impact of the sensor time lag error is discussed in Miloshevich et al. (2001). In section 6b, we also give several site specific errors, such as the nighttime condensation errors on R/V *Kexue* and at Kavieng.

6. Application to TOGA COARE data and validation

a. Corrections of TOGA COARE data

The correction algorithm using the sonde age in Fig. 10 is applied to 4010 non-NCAR RS80 soundings (Table

TABLE 3. Uncertainties in humidity corrections at conditions of T = 27°C and RH = 80% for a 0.96-yr-old RS80-A sonde.

Types of corrections	Corrections	Uncertainties absolute (relative to corrections)	Explanations
Age (yr)	0.96	Δage: 0.48 (50%)	Introducing 50% uncertainties in assumed ages
Contamination (dry bias)	C_{CA}: 1.73	$\Delta C_{CAmodel}$: 1.55 (90%)	1.55% uncertainties in C'_{CA} from the lab test
		ΔC_{CAage}: 0.64 (37%)	Uncertainties due to 50% uncertainties in age
Basic calibration model	C_{MA}: −1.77	$\Delta C_{MAmodel}$: 0.9 (51%)	0.9% uncertainties in C'_{MA} from the lab test
TD	C_{TA}: −0.68	ΔC_{TA}: 0	No lab tests for $T>$ 0°C, so no uncertainties from model
Modeled ground check	C_{GC}: 0.74	$\Delta C_{GCmodel}$: 0.6 (81%)	0.6% uncertainties in C_{GC} from the lab test
		ΔC_{GCage}: 0.29 (39%)	Uncertainties due to 50% uncertainties in age
SAH	C_{SAH}: 4.57	$\Delta C_{SAHmodel}$: 3.01 (66%)	Uncertainties in the SAH correection model (see Fig. 7). A surface RH of 85% is assumed to calculate C_{SAH}
Total	C_{TOT}: 4.58	ΔC_{TOT}: 6.99 (153%)	The sum of all uncertainties
		ΔC_{TOTage}: 0.93 (20%)	Total uncertainty due to uncertainties in age
		$\Delta C_{TOTmodel}$: 6.06 (133%)	Total uncertainty due to uncertainties in models
Total after removing C_{MA}	$C_{TOTrmCma}$: 6.35	ΔC_{TOT}: 6.09 (96%)	The sum of all uncertainties
		ΔC_{TOTage}: 0.93 (15%)	Total uncertainty due to uncertainties in age
		$\Delta C_{TOTmodel}$: 5.16 (81%)	Total uncertainty due to uncertainties in models

1) C_{CA}, C_{MA}, $\Delta C_{CAmodel}$, ΔC_{CAage} and $\Delta C_{MAmodel}$ have been corrected back for temperature dependence of humdity sensor, i.e., C_{CA} in the table is $C'_{CA}/f(t)$, where $f(t)$ = 0.99963 + (1.83105E−5)t. However, at T = 27°C, $f(t)$ is very small (0.000098).

2) C_{SAH} and $\Delta C_{SAHmodel}$ are values at surface (maximum values). The SAH corrections are only applied from 10 to 50 s by $(C_{SAH})e^{-time/13}$.

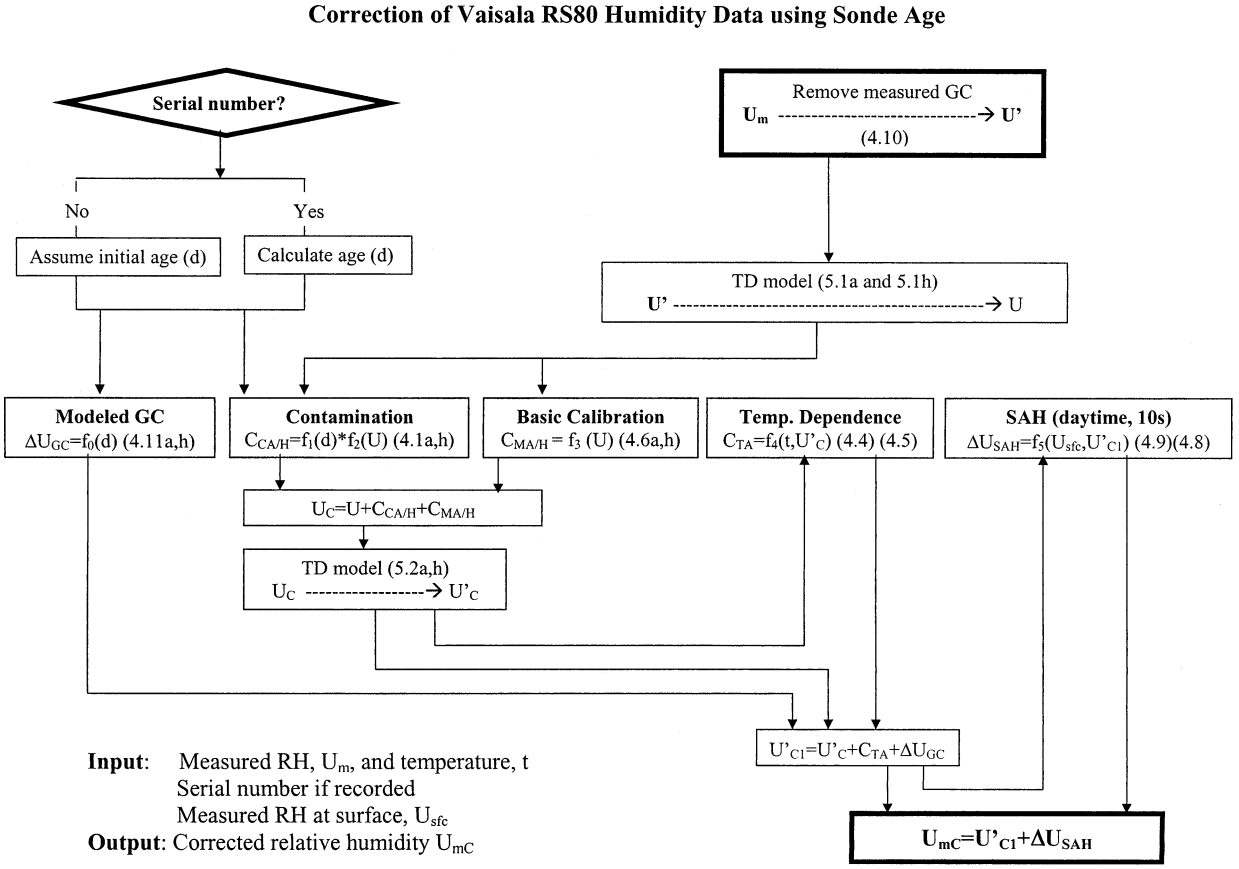

FIG. 10. Overview of the correction algorithm using the sonde age (see the text for details). The numbers in parentheses are equation numbers listed in text (with a in the figure equivalent to A in the text and h equivalent to H).

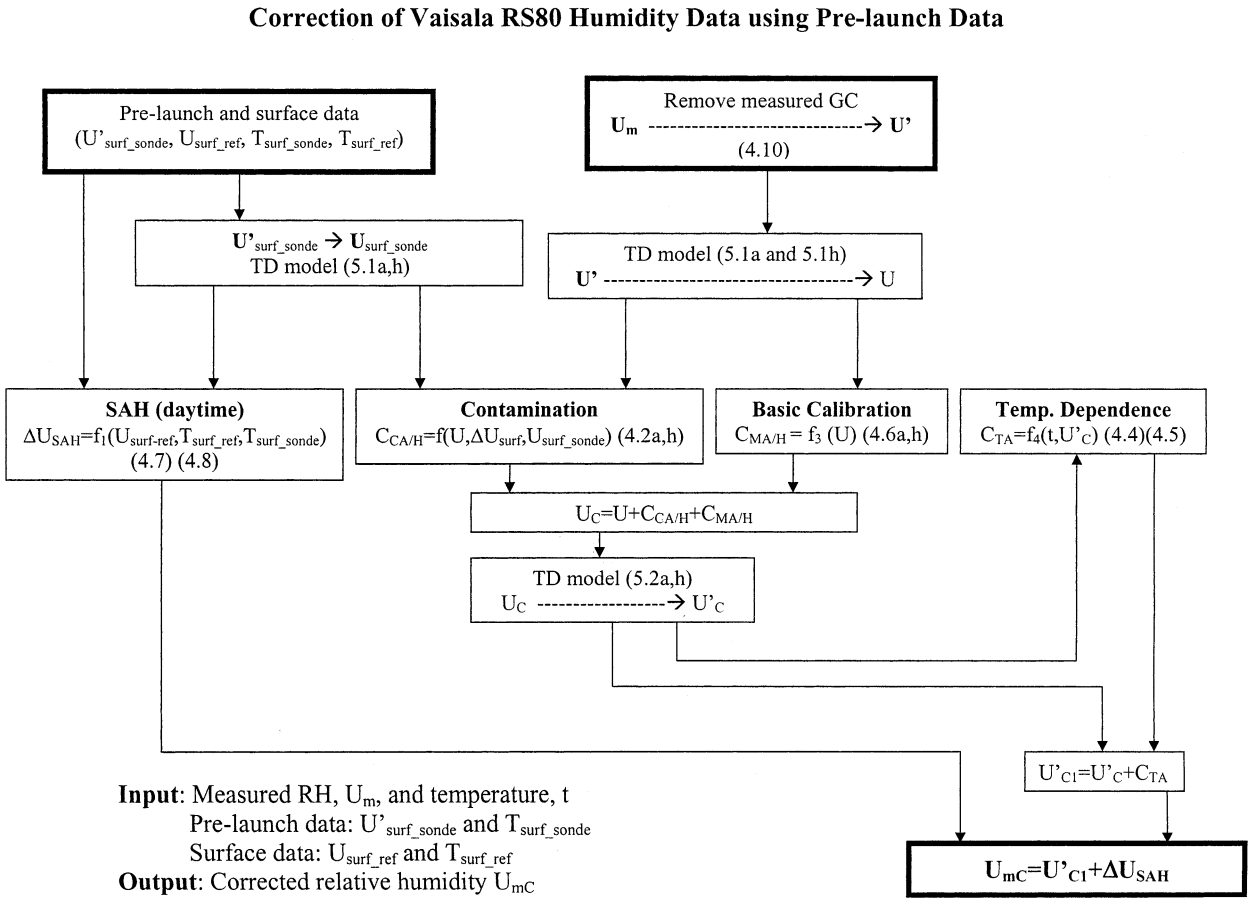

FIG. 11. Overview of the correction algorithm using the prelaunch data (see the text for details). The numbers in parentheses are equation numbers listed in text (with a in the figure equivalent to A in the text and h equivalent to H).

TABLE 4. Uncertainties in humidity corrections at conditions of T = 27°C and RH = 80% for a 1.25-yr-old RS80-H sonde.

Types of corrections	Corrections	Uncertainties absolute (relative to corrections)	Explanations
Age (yr)	1.25	Δage: 0.625 (50%)	Introducing 50% uncertainties in assumed ages
Contamination (dry bias)	C_{CH}: 6.64	$\Delta C_{CHmodel}$: 0.55 (8%)	0.55% uncertainties in C'_{CA} from the lab test
	ΔC_{CHage}: 0.6 (9%)	Uncertainties due to 50% uncertainties in age	
Basic calibration model	C_{MH}: −0.12	$\Delta C_{MHmodel}$: 0.35 (285%)	0.35% uncertainties in C'_{MH} from the lab test
TD	C_{TH}: −1.25	ΔC_{TH}: 0	No lab tests for $T>$ 0°C, so no uncertainties from model
Modeled ground check	C_{GC}: 1.33	$\Delta C_{GCmodel}$: 0.99 (74%)	0.99% uncertainties in C_{GC} from the lab test
		ΔC_{GCage}: 0.57 (43%)	Uncertainties due to 50% uncertainties in age
SAH	C_{SAH}: 3.36	$\Delta C_{SAHmodel}$: 3.01 (89%)	Uncertainties in the SAH correction model (see Fig. 7). A surface RH of 87% is assumed to calculate C_{SAH}
Total	C_{TOT}: 9.96	ΔC_{TOT}: 6.07 (61%)	The sum of all uncertainties
		ΔC_{TOTage}: 1.17 (12%)	Total uncertainty due to uncertainties in age
		$\Delta C_{TOTmodel}$: 4.9 (49%)	Total uncertainty due to uncertainties in models
Total after removing C_{MA}	$C_{TOTrmCmh}$: 9.84	ΔC_{TOT}: 5.72 (58%)	The sum of all uncertainties
		ΔC_{TOTage}: 1.17 (12%)	Total uncertainty due to uncertainties in age
		$\Delta C_{TOTmodel}$: 4.55 (46%)	Total uncertainty due to uncertainties in models

1) C_{CH}, C_{MH}, ΔC_{CHage} and $\Delta C_{MHmodel}$ have been corrected back for temperature dependence of humidity sensor [see Eqs. (5.2-A) and (5.2-H)].

2) C_{SAH} and $\Delta C_{SAHmodel}$ are values at surface (maximum values). The SAH corrections are only applied from 10 to 50 s by $(C_{SAH})e^{-\text{time}/13}$.

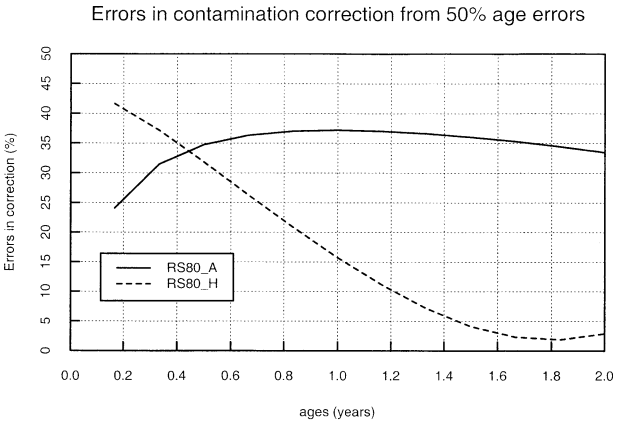

FIG. 12. Relative errors in contamination correction due to 50% errors in ages as a function of sonde ages for RS80-A and RS80-H.

1), and the correction algorithm using the prelaunch data in Fig. 11 is used to correct 4119 NCAR soundings. The mean correction at 17 non-NCAR RS80-A sites is about 1.7% in the lower and middle troposphere and increases in the upper troposphere because of the significant TD correction at cold temperatures (Fig. 13). The mean correction for the RS80-H is about twice as large as that for the RS80-A in the lower and middle troposphere, but is much smaller than that for the RS80-A in the upper troposphere because of smaller TD corrections for the RS80-H. The SAH correction contributes to increased corrections near the surface during the daytime.

The actual ages determined from serial numbers were used for the contamination correction at Darwin, Gove, *Vickers*, *Hakuho Maru*, Misima, and Thursday Island. Sondes used at these six stations were manufactured 2 $\sim$ 3 months in advance (Misima, Thursday Island, and *Vichers*) or 5 $\sim$ 7 months (Darwin and Gove), and different batches of sondes were used at one site (*Hakuho Maru*, not shown). Based on this, we assume that all sondes were manufactured four months before the first day of the experiment (1 November 1992) at those stations without recorded serial numbers. As the result, sonde ages are increased from 4 to about 8 months at the end of IOP (28 February 1993). A 50% error in age introduces less than a 45% error in the contamination correction at 50% RH for all sondes younger than 2 yr old (Fig. 12).

b. Site-specific factors

During COARE corrections and subsequent evaluations of the corrected data, we encountered several site- and time-specific problems. Several major specific problems related to corrections for the COARE data are listed below.

We corrected contamination errors for the NCAR data using the surface RH difference from the surface instrument and prelaunch radiosonde measurements [see

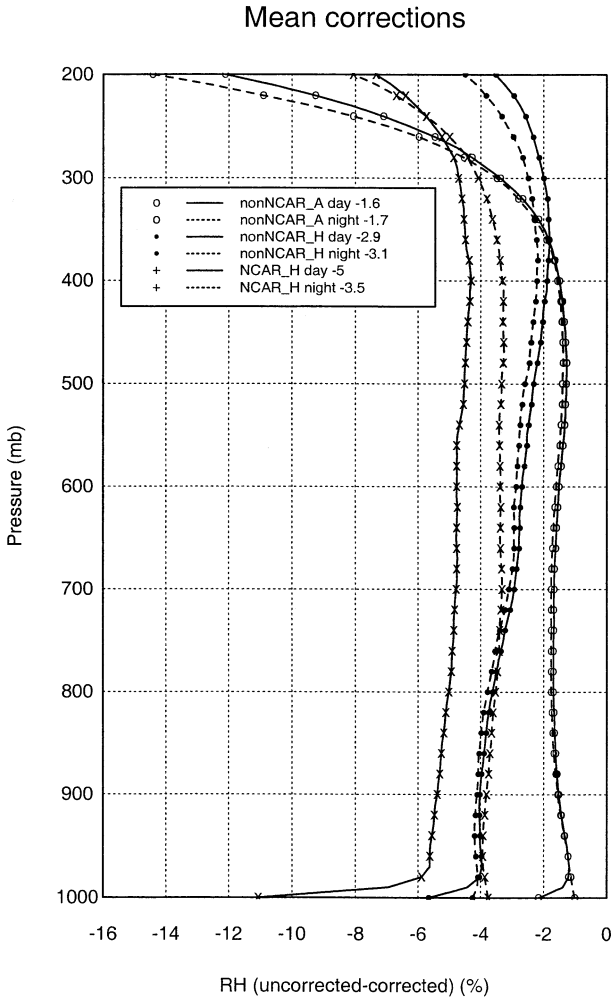

FIG. 13. Vertical profiles of mean RH differences (%) between uncorrected and corrected data at day and night averaged for all non-NCAR RS80-A soundings (non-NCAR A), all non-NCAR RS80-H soundings (non-NCAR H), and all NCAR RS80-H soundings (NCAR H) during IOP. The mean values averaged from 1000 to 300 mb are given in the legend.

Eqs. (4.2-A) and (4.2-H)]. The accuracy of this correction method depends on the accuracy of the surface RH measured by the independent surface instrument, which was the Vaisala HMP-35 mounted in a ventilated radiation shield at the NCAR COARE sites. The comparison of the surface RH measured by the HMP-35 and a wet–dry-bulb psychrometer at Manus shows that the HMP-35 RH sensor has a small dry bias at RHs above $\sim$88%. This dry bias has been verified by Vaisala based on their quality tests of HMP-35 sensor (L. Stormbom, Vaisala, 1999, personal communication). The dry bias is as high as 3% at 100% RH, and varies more or less linearly from 0% at 88% RH to 3% at 100% RH. We apply a linear correction to the HMP-35 measured surface RH between 88% and 97% with no change made at 88% and a 3% correction at 97% RH. This surface RH correction was applied to all soundings (day and

night) at all NCAR stations except the R/V *Xiang-YangHong* (ship 5) where another type of surface humidity sensors was used and the *Moana Wave* where the surface data were corrected and supplied by the National Oceanic and Atmospheric Administration (NOAA) Environmental Technology Laboratory (ETL).

The summary plot of the MR difference at all sites in Fig. 2 shows a small MR difference on the R/V *Kexue* (sc1) and at Kavieng, and a large difference at Santa Cruz. On the R/V *Kexue* and at Kavieng, we believe that condensation would occur on the sensor at night when sondes were moved to the warm and humid outside from the cold air-conditioned storage room. Therefore, these sondes measured higher humidity values than actual values. For these two stations, we assign negative ΔU_{surf} in Eqs. (4.2-A) and (4.2-H) to be zero, that is, no correction is made. The large MR difference at Santa Cruz is due to the large daytime value of MR difference (5.37 g kg^{-1} during the daytime versus 2.82 g kg^{-1} at night). The value of 5.37 g kg^{-1} MR difference during the daytime is a result of the large surface MR (20.7 g kg^{-1}). The warm surface temperature (mean: 30.37°C) might cause such a large surface MR. Such warm daytime surface temperature is either real or artificial due to inadequately ventilated surface temperature sensor. Because we cannot determine which one is right, we can only annotate the data as questionable.

The algorithm using the prelaunch measurements for the NCAR RS80-H data gives a larger correction during the daytime than the algorithm using the sonde age for the non-NCAR RS80-H data, but two algorithms produce similar corrections in magnitude during the nighttime (Fig. 13). The day–night difference of the RH correction for the NCAR data only exists at four island stations (Kapinga, Kavieng, Manus, and Nauru). Our analyses of day–night difference show that dry biases in the HMP–35 surface measurements and nighttime condensation contribute partly to this difference. After correcting the HMP–35 dry biases, the day–night difference is reduced but still exists in a significant magnitude at Kavieng, Manus, and Nauru. Nighttime condensation occurred at Kavieng has not been (and cannot be) corrected at this point. Further investigation needs to be done to understand this day–night difference.

For the NCAR soundings, the SAH error was corrected using the prelaunch sonde temperature and HMP-35 measured surface temperature and RH [see Eq. (4.7)]. This SAH correction was applied to daytime soundings at all NCAR stations except Nauru and Kapinga. At both Nauru and Kapinga, radiosondes were launched from an air-conditioned enclosure; that is, the prelaunch data represent the condition inside the enclosure that was both cooler and drier than the ambient air. In addition, the air-conditioned launch also affects the contamination correction using the prelaunch data. For these stations, we estimated the dry bias at the surface (ΔU_{surf}) using the prelaunch RH value in the launcher itself and the measured ambient RH value outside the launcher along with the radiosonde RH sensor response time.

The SAH correction in Eq. (4.9) is applied to all daytime non-NCAR soundings with 10-s resolution. We recognize that the SAH does not necessarily occur at all stations and all conditions. For instance, it depends on whether a balloon inflation shelter was used, and whether it was clear or cloudy. However, there is no quantitative way to determine presence or absence of SAH effects. Our experience during TOGA COARE suggests that SAH occurred at most sites. SAH correction has a large impact compared to other correction factors near the surface, and the SAH model uncertainty is smaller in relative values than that for contamination and the modeled GC corrections. Therefore, we apply SAH corrections uniformly to all stations whenever the correction algorithm is applicable; that is, it is daytime, 10-s data, and $\Delta \text{RH}_{10s} > 0$. We acknowledge that the SAH correction might introduce some errors rather than correcting for a nonexistent SAH error if there are thick clouds or rain falling during daytime.

c. Validation

After making corrections, each sounding was examined for ''reasonableness'' based on individual skew-*T* plot analysis. Any obvious glitches were changed to missing values. Various summary plots were generated at each station for both day and night soundings to evaluate the performance of correction algorithms, including scatterplots of comparisons between the surface MR from independent surface instruments and averaged MR at the top of the mixed layer from radiosonde data before and after corrections, vertical profiles of mean and standard deviation of corrections, and histograms of convective available potential energy (CAPE) and RH before and after corrections. Figure 14 shows the validation plots for soundings at Kavieng. After corrections, the MR differences range from 0 to 2 g kg^{-1} for most of the soundings with a mean value of 0.7 g kg^{-1}, which is more consistent with what might be expected for a maritime tropical environment. The majority (84%) of corrected soundings have CAPE values above 800 J kg^{-1}. The corrected soundings also show more RH values above 90%. The skew-*T* plot with a corrected dew point sounding on 5 January 1993 is also shown in Fig. 14. The corrected dewpoint trace shows two saturated layers, one at 850–750 mb and the other at 600–500 mb, indicating two cloud layers. In general, corrected soundings at all stations look ''reasonable'' based on these validation results.

The surface-sonde MR differences after corrections are decreased by 0.4 and 1.13 g kg^{-1} on average at RS80-A and RS80-H stations, respectively (Fig. 2). After corrections, the frequency of soundings with CAPE values larger than 800 J kg^{-1} increases by 5%–40%, and is above 70% at all eight NCAR stations (Fig. 3). Note that the MR difference and the fraction of CAPE

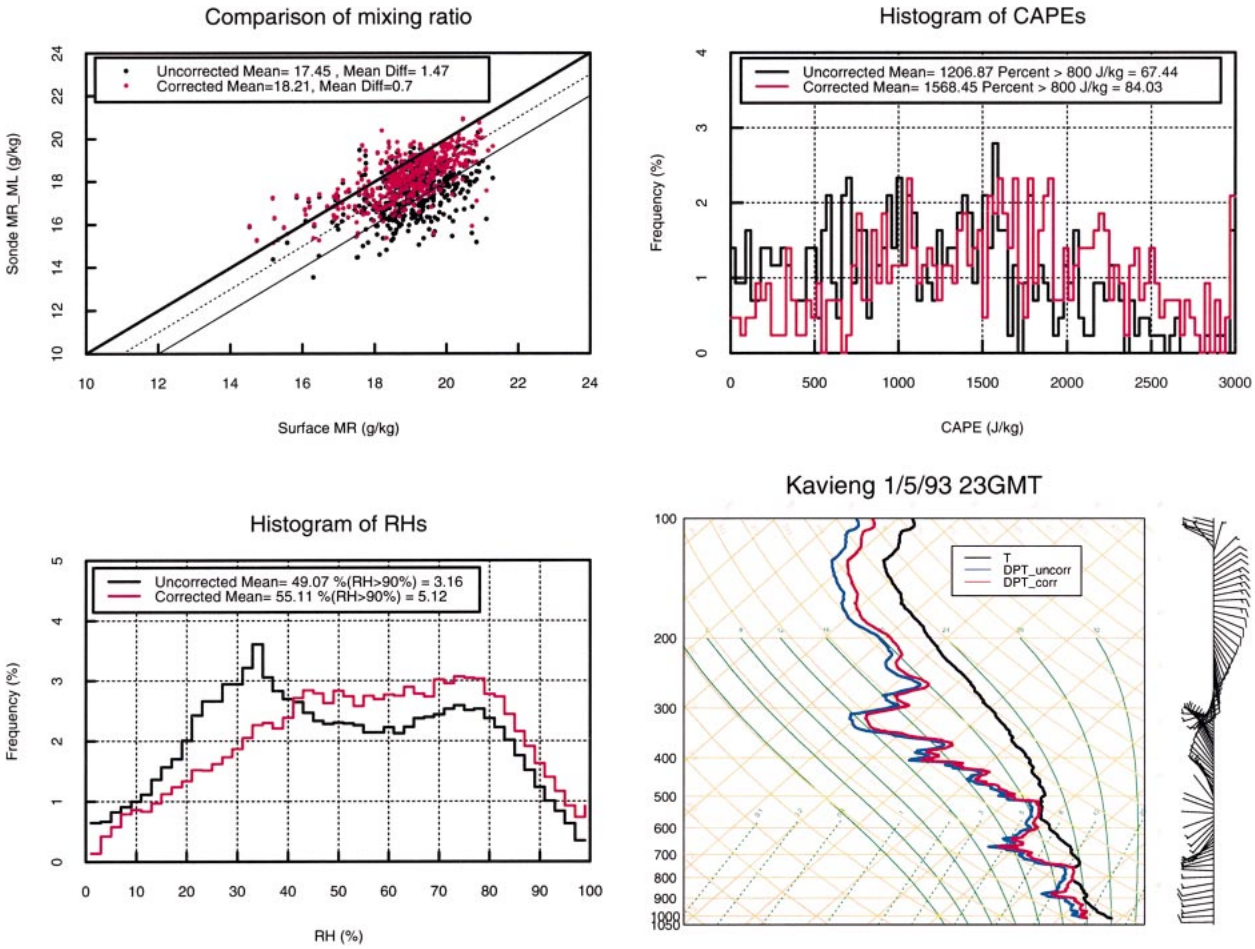

FIG. 14. (top left) Scatterplot of surface MR vs radiosonde-measured mean mixed-layer MR, histograms of (top right) CAPES and (bottom left) RHs, and (bottom right) skew-*T* plot of the sounding at Kavieng (5 Jan 1993, 2300 UTC), both before and after corrections.

> 800 J kg^{-1} are expected to vary from one station to another one. Figure 4 shows that after corrections high humidity values at low levels extend from 5°N to 5°S; midlevel moisture values at the south of 5°N have also increased while the dry intrusions at 700 mb show in sharper details; RH above 400 mb at the south of 5°N has increased substantially (due primarily to TD corrections).

After corrections there are improvements in MR differences, CAPE values, and mean RH profiles (Figs. 2, 3, 4). However, the corrections using the sonde age are still much smaller than the corrections using the prelaunch radiosonde data (diamonds in Fig. 2). The method using surface data as an independent reference corrects not only the contamination error but also other errors that contribute to the differences between the surface-sensor-measured and radiosonde-measured surface RH. The age method gives the same contamination correction for all sondes with the same ages, and is unable to account for variations in the sondes within batches and any batch-to-batch differences.

These correction methods can also be evaluated by comparing corrected data with other independent data, and were tested against microwave radiometer measurement for the RS80-H in the ARM program (Liljegren et al. 1999). A comparison of simultaneous RH measurements from the RS80-A and the NOAA cryogenic frost point hygrometers shows that corrected RS80-A RH profiles correspond well with the hygrometer profiles, and also shows RH values near or above ice saturation inside cirrus clouds indicated by the hygrometer data (Miloshevich et al. 2001; Wang et al. 2001a). In January 2000 in Helsinki, Finland, Vaisala launched balloons carrying dual radiosondes (RS80-A vs RS80-H, and RS80 vs RS90). We compared the RS80-A data with the RS80-H and RS90 sounding data. These RS80 soundings were free of contamination errors because they were stored in an environment without any contamination. Figure 15 shows two examples. For sounding 3163, the RS80-A RH profile after correction is more closely in agreement with the RS80-H sounding, and shows a supersaturation layer at 340–250 mb identified by the RS80-H data (Fig. 15 left). The RS90 data have higher accuracy and faster response time than the

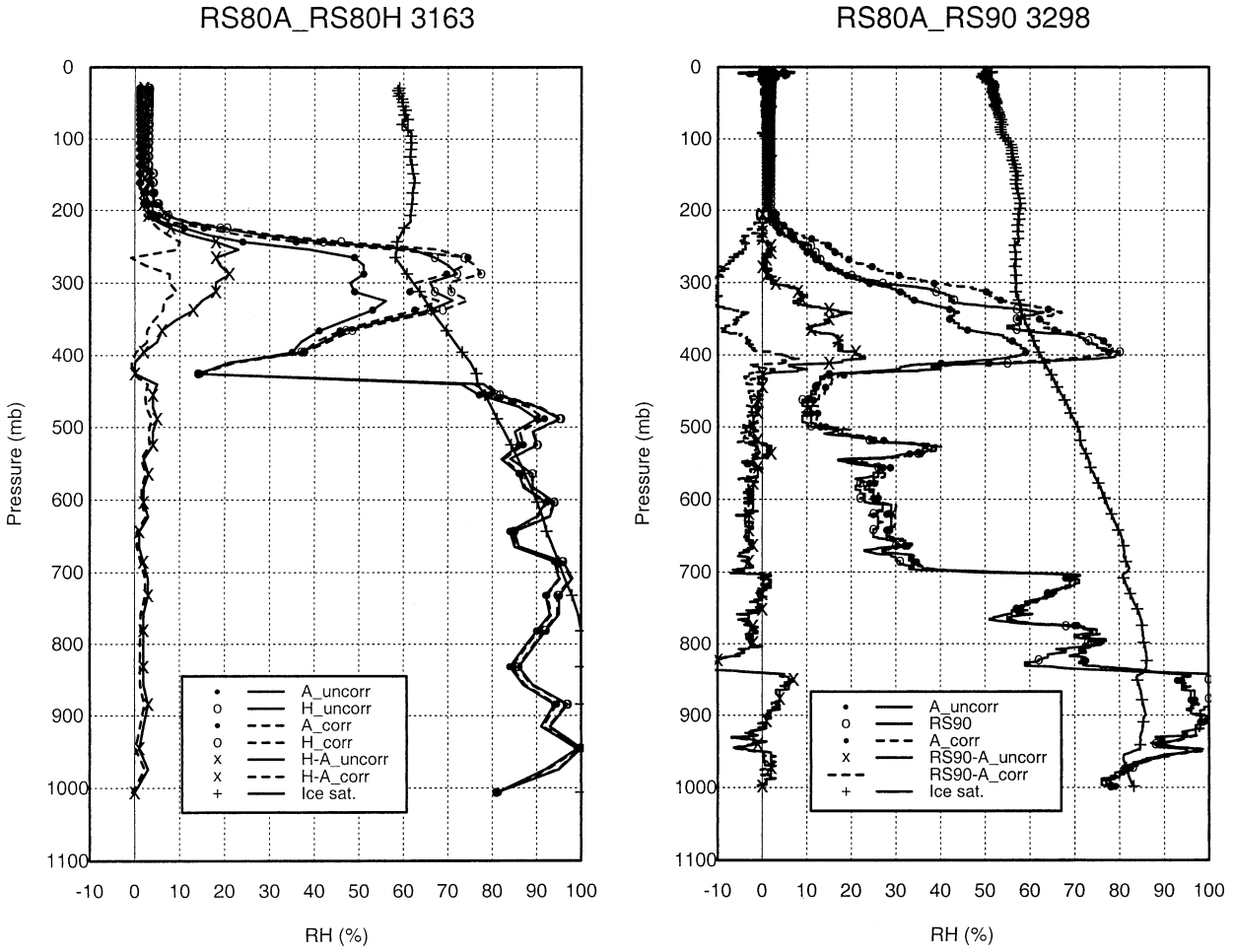

FIG. 15. Comparison of RH profiles form uncorrected and corrected (left) RS80-A and RS80-H data for sounding 3163, and (right) uncorrected RS80-A and RS90 data for sounding 3298. The profiles of RH differences and ice saturation are also shown.

RS80, and can be used as a reference. For sounding 3298, the difference between the RS90 and the RS80-A is reduced from 10%–20% to −10%–0% in the 400–300-mb layer after correction, and the corrected RS80-A RH profile reveals a super-saturation cloud layer in the 400–300-mb layer (Fig. 15 right). The higher RS80-A measured RH values above cloud top than those measured by the RS90 is due to the RS80's slower sensor response time than the RS90, suggesting the need for correction of sensor time lag errors.

7. Summary and significance

A consistent dry bias in the TOGA COARE Vaisala RS80 humidity data was revealed by several indicators, such as much drier boundary layers measured by radiosonde data than the surface humidity measured by reference sensors, lack of CAPE values large enough for convective initiation, and lack of saturation layers indicating clouds. Working together in field data and laboratory data, NCAR/ATD and Vaisala have worked to understand the dry bias error along with five other errors in Vaisala RS80 humidity data and have developed general methods for correcting them. The six errors are 1) a contamination error, 2) a temperature-dependence error, 3) a basic-calibration-model error, 4) a ground-check error, 5) a sensor-aging error, and 6) a sensor-arm-heating error. Correction methods developed for the first five errors are based on the data from a series of laboratory tests run at Vaisala. The SAH correction method for non-NCAR soundings is a statistical approach derived from COARE NCAR soundings where the SAH correction is calculated from prelaunch radiosonde data. The implementation of all the correction methods is summarized in Figs. 10 and 11 and forms the overall correction model. The correction model uses input values from radiosonde-measured RH and temperature profiles, surface RH and temperature measurements by independent surface sensors, radiosonde serial numbers (if recorded), and the radiosonde data prior to launch (prelaunch data) if available. For the correction algorithm using the sonde age, the age is

determined from the sonde serial number, or can be estimated by assuming one fixed sonde manufacture date if the serial numbers were not recorded. The output of the correction model is corrected RH profiles (Figs. 10 and 11).

The correction algorithm was applied to all 8129 COARE Vaisala RS80 soundings and was evaluated by examining various summary plots. Our evaluation shows that the corrected humidity data are generally ''reasonable.'' We expect that subsequent uses of the corrected dataset will confirm its improved accuracy from the uncorrected data. The correction methods presented in this paper bear uncertainties, and the uncertainty is analyzed and presented in section 5b. Total uncertainty is smaller than total correction for both the RS80-A and the RS80-H. We have tried to highlight remaining uncertainties from correction methods and from site-specific factors in the TOGA COARE dataset to guide future users.

We see several significant outcomes of our joint work. Vaisala changed the desiccant type in the package from clay to the mixture of active charcoal and silica gel in September 1998 and also introduced a new type of protective shield over the sensor boom in May 2000 for RS80 sondes (see section 4a). The protective cover with desiccant is expected to prevent the contamination completely. Second, this work makes the corrected COARE radiosonde dataset one of the most examined and highest quality radiosonde datasets ever collected. The correction process substantially reduces errors in radiative and thermodynamical parameters and atmospheric heat and moisture budgets derived from the COARE radiosonde data (Guichard et al. 2000; Johnson and Ciesielski 2000). Potentially, it can improve the precipitation and cloud predictions for numerical weather prediction models (Lorenc et al. 1996). Third, although the correction methods have been developed for COARE data, they are applicable to any RS80 radiosonde data. For example, the contamination and TD corrections have been applied to various radiosonde datasets and have led to a better agreement in the upper-tropospheric humidity (UTH) between the RS80 data and other independent measurements, suggesting increased accuracy of Vaisala RS80 UTH data after corrections (Wang et al. 2001a). Our correction methods can also be applied to historical and global radiosonde datasets to reduce or eliminate temporal and spatial inhomogeneity associated with Vaisala humidity errors and thus significantly enhance the usefulness of those datasets for studying of long-term water vapor variations (e.g., Wang et al. 2001b). These correction methods could become an effective tool for recalculation of sounding data from field experiments and historical radiosonde data and in European Centre for Medium-Range Weather Forecasts (ECMWF) and NCAR/National Centers for Environmental Prediction (NCEP) global reanalysis efforts. Note that in order to use correction methods described in this paper, RS80-A sondes have to be manufactured after October 1985 when the last temperature dependence correction was done, and before September 1998 when Vaisala changed the desiccant type in the package. Finally, we now believe that corrected Vaisala humidity data can be considered as a reliable reference and can help in developing correction methods for other archived radiosonde datasets.

We learn from this study that besides instrumental errors and biases, practices in storing, handling, and releasing radiosondes before launch can introduce significant errors/biases to data too, such as ground-check error and the moist bias due to nighttime condensation effect. We appeal for careful examinations of special practices in storing, handling and releasing radiosondes before those practices are used in the field experiments. For the GC, we suggest that a consistent and strict guideline for operating the GC device should be made for all radiosonde stations and all field experiments. Evaluations of our correction methods show that better results were achieved using prelaunch data than using sonde age. A prelaunch RH measurement from the radiosonde is required for the contamination correction method using prelaunch data and was only available for radiosonde data from some field experiments, such as NCAR COARE data described in this paper. We recommend recording radiosonde data prior to launch as a mandatory practice for all operational and reseach radiosonde releases. Comparisons of prelaunch radiosonde data with the surface data from independent surface sensors can always be used to evaluate the accuracy of radiosonde data (and/or surface data), and may provide some guidance on how to correct the data. It is possible that Vaisala can modify their data acquisition system to record prelaunch data automatically. Radiosonde serial number is used to estimate the sonde age for correcting the contamination dry bias and the sensor aging error in our correction methods. The serial number provides production information on sondes, and also helps us to investigate bath-to-batch differences. However, it is not always recorded. We appeal for recording radiosonde serial number for all operational and research radiosonde launches.

Acknowledgments. We would like to thank Alan Sharp and Scot Loehrer for providing serial number and ground-check data at six stations, Tim Hoar for making Vaisala dual-launch radiosonde data available, and David Parsons and Larry Miloshevich for useful discussions. J. Wang is grateful to Doug Nychka, Tim Hoar, and Eric Gilleland for help in statistics and S-plus. This work is supported by special NSF/ATM and NOAA/OGP funding to ATD.

REFERENCES

Antikainen, V., and A. Paukkunen, 1994: Studies on improving humidity measurements in radiosondes. *Proc. WMO Tech. Conf.*

on Instruments and Methods of Observation, Geneva, Switzerland, WWW/OSY, WMO/TD 588, 137–141.

Cole, H., and E. Miller, 1995: A correction for low-level radiosonde temperature and relative humidity measurements. Preprints, *Ninth Symp. on Meteorological Observations and Instrumentation,* Charlotte, NC, Amer. Meteor. Soc., 32–36.

Fairall, C. W., E. F. Bradley, D. P. Rogers, J. B. Edson, and G. S. Young, 1996: Bulk parameterization of air–sea fluxes for Tropical Ocean–Global Atmosphere Coupled Ocean–Atmosphere Response Experiment. *J. Geophys. Res.,* **101,** 3747–3764.

Ferrare, R. A., S. H. Melfi, D. N. Whiteman, K. D. Evans, F. J. Schmidlin, and D. O'C. Starr, 1995: A comparison of water vapor measurements made by Raman lidar and radiosondes. *J. Atmos. Oceanic Technol.,* **12,** 1177–1195.

Guichard, F., D. Parsons, and E. Miller, 2000: Thermodynamical and radiative impact of the correction of sounding humidity bias in the Tropics. *J. Climate,* **13,** 3611–3624.

Johnson, R. H., and P. E. Ciesielski, 2000: Rainfall and radiative heating from TOGA COARE atmospheric budgets. *J. Atmos. Sci.,* **57,** 1497–1514.

Kostamo, P. J., 1989: RS 80 radiosonde ground check corrections of temperature. *Vaisala News,* **117-118/89,** 3–7.

LeMone, M., E. J. Zipser, and S. Trier, 1998: The role of environmental shear and thermodynamic conditions in determining the structure and evolution of mesoscale convective systems during TOGA COARE. *J. Atmos. Sci.,* **55,** 3493–3518.

Lesht, B. M., 1999: Reanalysis of radiosonde data from the 1996–1997 water vapor intensive observation periods: Application of the Vaisala RS-80H contamination correction algorithm to dual-sonde soundings. *Proc. Ninth Atmospheric Radiation Measurement (ARM) Program Science Team Meeting,* San Antonio, TX, Dept. of Energy. [Available online at http://www.arm.gov/docs/documents/technical/conf_9903/lesht-99.pdf.]

Liljegren, J. C., B. M. Lesht, T. Van Hove, and C. Rocken, 1999: A comparison of integrated water vapor from microwave radiometer, balloon-borne sounding system and global positioning system. *Proc. Ninth Atmospheric Radiation Measurement (ARM) Program Science Team Meeting,* San Antonio, TX, Dept. of Energy. [Available online at http://www.arm.gov/docs/documents/technical/conf_9903/liljegren(3)-99.pdf.]

Lorenc, A. C., D. Barker, R. S. Bell, B. Macpherson, and A. J. Maycock, 1996: On the use of radiosonde humidity observations in mid-latitude NWP. *Meteor. Atmos. Phys.,* **60,** 3–17.

Lucas, C., and E. J. Zipser, 2000: Environmental variability during TOGA COARE. *J. Atmos. Sci.,* **57,** 2333–2350.

Matsuguchi, M., Y. Umeda, and Y. Sakai, 1998: Characterization of polymers for a capacitive-type humidity sensor base on water absorption behavior. *Sens. Actuators,* **49,** 179–185.

Miloshevich, L. M., H. Vomel, A. Paukkunen, A. J. Heymsfield, and S. J. Oltmans, 2001: Characterization and correction of relative humidity measurements from Vaisala RS80-A radiosondes at cold temperatures. *J. Atmos. Oceanic Technol.,* **18,** 135–155.

Parsons, D., and Coauthors, 1994: The Integrated Sounding System: Description and preliminary observations from TOGA COARE. *Bull. Amer. Meteor. Soc.,* **75,** 553–566.

Ross, R. J., and D. J. Gaffen, 1998: Comment on ''Widespread tropical atmospheric drying from 1979 to 1995'' by Schroeder and McGuirk. *Geophys. Res. Lett.,* **25,** 4357–4358.

Salasmaa, E., and P. Kostamo, 1975: New thin film humidity sensor. Preprints, *Third Symp. on Meteorological Observations and Instrumentation,* Washington, D.C., Amer. Meteor. Soc., 33–38.

Schroeder, S. R., and J. P. McGuirk, 1998: Widespread tropical atmospheric drying from 1979 to 1995. *Geophys. Res. Lett.,* **25,** 1301–1304.

Soden, B. J., and J. R. Lanzante, 1996: An assessment of satellite and radiosonde climatologies of upper-tropospheric water vapor. *J. Climate,* **9,** 1235–1250.

Wang, J., W. Brown, D. J. Carlson, H. L. Cole, E. R. Miller, D. B. Parsons, and K. Yoneyama, 2000: Ground check corrections in radiosonde data on the R/V Mirai during Nauru99. *Proc. Tenth Atmospheric Radiation Measurement (ARM) Program Science Team Meeting,* San Antonio, TX, Dept. of Energy. [Available online at http://www.atd.ucar.edu/homes/junhong/paper/eabs-arm00.htm.]

——, H. L. Cole, D. J. Carlson, and A. Paukkunen, 2001a: Performance of Vaisala RS80 radiosonde on measuring upper-tropospheric humidity after corrections. Preprints, *Eleventh Symp. on Meteorological Observations and Instrumentation,* Albuquerque, NM, Amer. Meteor. Soc., 94–97.

——, ——, and ——, 2001b: Water vapor variability in the tropical western Pacific from 20-year radiosonde data. *Adv. Atmos. Sci.,* **18,** 752–766.

Webster, P. J., and R. Lukas, 1992: TOGA COARE: The Coupled Ocean–Atmosphere Response Experiment. *Bull. Amer. Meteor. Soc.,* **73,** 1377–1416.

Zipser, E. J., and R. H. Johnson, 1998: Systematic errors in radiosonde humidities a global problem? Preprints, *10th Symp. on Meteorological Observations and Instrumentation,* Phoenix, AZ, Amer. Meteor. Soc., 72–73.